ACS chemical biology

Articles

pubs.acs.org/acschemicalbiology

A Hydrogel-Microsphere Drug Delivery System That Supports Once-Monthly Administration of a GLP-1 Receptor Agonist

Eric L. Schneider,[†] Brian R. Hearn,[†] Samuel J. Pfaff,[†] Ralph Reid,[†] David G. Parkes,[‡] Niels Vrang,[§] Gary W. Ashley,[†] and Daniel V. Santi*[,†,∥]

[†]ProLynx, 455 Mission Bay Blvd. South, Suite 145, San Francisco, California 94158, United States

[‡]DGP Scientific Inc., Del Mar, California 92014, United States

[§]Gubra ApS, Horsholm Kongevej 11B, 2970 Horsholm, Denmark

[∥]Department of Pharmaceutical Chemistry, University of California, San Francisco, 600 16th Street, San Francisco, California 94158, United States

Supporting Information

ABSTRACT: We have developed a chemically controlled very long-acting delivery system to support once-monthly administration of a peptidic GLP-1R agonist. Initially, the prototypical GLP-1R agonist exenatide was covalently attached to hydrogel microspheres by a self-cleaving β-eliminative linker; after subcutaneous injection in rats, the peptide was slowly released into the systemic circulation. However, the short serum exenatide half-life suggested its degradation in the subcutaneous depot. We found that exenatide undergoes deamidation at Asn^{28} with an *in vitro* and *in vivo* half-life of approximately 2 weeks. The [Gln^{28}]exenatide variant and exenatide showed indistinguishable GLP-1R agonist activities as well as pharmacokinetic and pharmacodynamic effects in rodents; however, unlike exenatide, [Gln^{28}]exenatide is stable for long periods. Two different hydrogel-[Gln^{28}]exenatide conjugates were prepared using β-eliminative linkers with different cleavage rates. After subcutaneous injection in rodents, the serum half-lives for the released [Gln^{28}]exenatide from the two conjugates were about 2 weeks and one month. Two monthly injections of the latter in the Zucker diabetic fatty rat showed pharmacodynamic effects indistinguishable from two months of continuously infused exenatide. Pharmacokinetic simulations indicate that the delivery system should serve well as a once-monthly GLP-1R agonist for treatment of type 2 diabetes in humans.

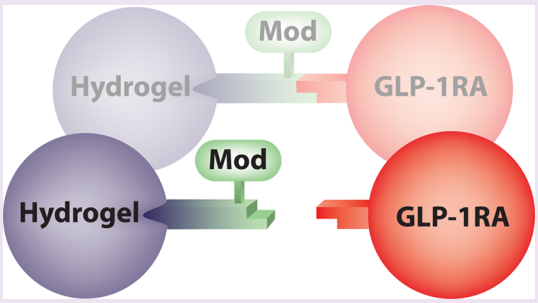

Peptidic GLP-1 receptor agonists (GLP-1RA) have emerged as an important standard-of-care drug class for the treatment of type 2 diabetes (T2D).[1] These agonists stimulate glucose-mediated insulin secretion, suppress inappropriately elevated glucagon secretion, and slow gastric emptying. Additionally, GLP-1RAs show potentially beneficial non-glycemic effects.[2,3] First, because they increase satiety and reduce food intake, they may have utility as antiobesity agents.[4−6] Second, as demonstrated for liraglutide[7] and semaglutide,[8] the drug class may reduce the risks for adverse cardiovascular events in patients with T2D.[9,10] Third, GLP-1RAs may prevent or ameliorate certain cognitive disorders[3] and, finally, as recently shown for liraglutide, may be efficacious in the treatment of nonalcoholic steatohepatitis.[11]

Exendin-4, a 39-amino acid peptide isolated from salivary secretions of the Gila monster, is the prototypical GLP-1RA.[12] Synthetic exenatide is marketed for treatment of patients with T2D as Byetta that—with an elimination half-life ($t_{1/2,\beta}$) of only ~2.5 h—requires twice daily subcutaneous (SC) injections. There is both demand for and benefit in longer-acting GLP-1RA delivery systems, and a number of once-daily and once-weekly (QW) administered agonists have been developed for treatment of T2D.[1,13] These longer-acting agonists show a greater reduction in fasting glucose and HbA1c than exenatide, a decreased incidence of nausea and vomiting, and improved patient convenience and compliance.[1] Nevertheless, poor medication adherence and persistence remain major contributing factors leading to failure of glycemic control in patients with T2D.[14] As observed with other chronic diseases, patient compliance and persistence in taking medications for T2D should improve as the dosing interval increases.[15−17] Thus, the development of even longer acting GLP-1RAs with increased convenience, compliance, persistence and, hopefully, therapeutic efficacy is a major and timely challenge.

Although no once-monthly (QM) GLP-1RAs have yet emerged, several attempts have been made to adapt QW agonists to longer-acting therapeutics. For example, the QW PLGA-encapsulated exenatide, Bydureon, has been reformulated as a suspension in medium-chain triglycerides for QM administration.[18] Although the QM suspension increased the

Received: March 14, 2017
Accepted: June 12, 2017
Published: June 12, 2017

DOI: 10.1021/acschembio.7b00218
ACS Chem. Biol. 2017, 12, 2107−2116

Scheme 1

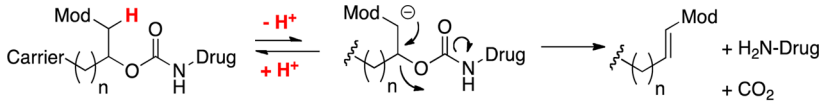

1 2 3

proportion of patients that achieved target HbA1c levels, the impracticably high viscosity of the formulation and its necessity for caregiver administration[19] will not address problems of compliance and persistence. Also, QW GLP-1 peptide agonist fusions of Fc,[20] albumin,[21] or XTEN[22,23] with half-lives of 5 to 6 days have been administered QM at doses sufficient to maintain therapeutic levels over multiple half-lives; here, the consequential high C_{max} and peak-to-trough (C_{max}/C_{min}) ratios >10 likely exceed tolerability limits. An ideal QM GLP-1RA would have a half-life of about one month, have a C_{max}/C_{min} within known tolerable limits, and be patient-administrable as a low-volume, painless SC injection using an autosyringe with a small bore needle. An implantable osmotic pump that efficiently delivers exenatide over six months is in clinical trials,[24] but patient acceptance of a surgically implanted device remains uncertain.

We have developed a general approach for half-life extension of therapeutics in which a drug is covalently tethered to a long-lived carrier by a linker that slowly cleaves to release the native drug.[25,26] Here, the linker is attached to a drug via a carbamate group (**1**; Scheme 1); the β-carbon has an acidic carbon−hydrogen bond (C−H) and also contains an electron-withdrawing "modulator" (Mod) that controls the pK_a of that C−H bond. Upon proton removal to give **2**, a rapid β-elimination occurs, cleaving the linker-carbamate bond and releasing the free drug. The rate of drug release is proportional to the acidity of the proton, which is controlled by the electron-withdrawing ability of the pK_a modulator. These linkers are not affected by enzymes and are stable for years when stored at low pH and temperatures.[25]

One carrier we use is a large-pore Tetra-PEG hydrogel polymer that presents little barrier to diffusion of released drugs.[26,27] These hydrogels are fabricated as uniform single-molecule ~40 μm microspheres by a microfluidic device[28] and can be easily injected SC through a small-bore needle. We also incorporate slower cleaving β-eliminative linkers in each of the cross-links of these polymers, so gel degradation can be adjusted to occur after drug release. Using linkers with different preprogramed cleavage rates to connect microspheres to drugs, the elimination half-lives of peptidic drugs have been increased from under 1 h to weeks or months.[28,29]

We previously reported a releasable Tetra-PEG hydrogel-exenatide conjugate that after SC administration provides systemic exenatide with a $t_{1/2,\beta}$ of ~7 days in the rat and should support QW administration of exenatide in humans.[28] This conjugate appears comparable to current QW GLP-1 agonists, but the several weekly agonists already on the market reduce the impetus for its clinical development.

In the present work, we describe experiments that led to the development of the first GLP-1 agonist that could be effectively administered by once-monthly SC administration in humans.

RESULTS

Pharmacokinetics of a Hydrogel-Exenatide Depot. Scheme 2 shows the three consecutive reactions that occur after

Scheme 2

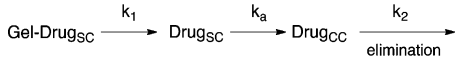

SC injection of noncirculating cleavable conjugates. The conjugate releases the drug by rate constant k_1 in the SC compartment ($Drug_{SC}$), which then enters the central compartment ($Drug_{CC}$) with k_a, from which it is eliminated with rate constant k_2. If, as in the present case, $k_2 > k_a > k_1$, the concentration of $Drug_{CC}$ at any time is described by eq 1, where CL is the drug clearance and F is the bioavailability.[28]

$$[\text{Drug}]_{CC,t} = \text{Dose} \times \frac{F}{\text{CL}} k_1 (e^{-k_1 t} - e^{-k_a t}) \quad (1)$$

We recently reported a releasable hydrogel-exenatide conjugate with a $MeSO_2$ modulator in the β-eliminative linker that showed a $t_{1/2,\beta}$ for released exenatide of 1 week in the rat.[28] We sought to increase the $t_{1/2,\beta}$ and studied a hydrogel having a linker with a −CN modulator designed to give ~4-fold slower drug release.[25]

We prepared N^{α}-[(7-azido-1-cyano-2-heptyloxy)carbonyl]-exenatide (N_3L[CN]-exenatide) by SPPS and attached it by strain-promoted alkyne−azide cycloaddition (SPAAC) to monofluorocyclooctyne (MFCO)-derivatized tetra-PEG hydrogels.[27,28] Under accelerated release conditions, the conjugate showed an extrapolated *in vitro* release $t_{1/2}$ of 2020 h at pH 7.4 and 37 °C.

Since *in vitro* release of exenatide from a β-eliminative linker is ~2-fold slower than *in vivo* release,[28] we anticipated an *in vivo* $t_{1/2,\beta}$ of ~1000 h for the released exenatide. However, a pharmacokinetic study of the SC hydrogel-exenatide conjugate in the rat showed a $t_{1/2,\beta}$ of only 240 h (Figure 1). Using eq 1, the expected $t_{1/2,\beta}$ of 1000 h, and pharmacokinetic parameters of exenatide in the rat,[30] we simulated the expected C vs t plot in the rat (Figure 1). The observed $t_{1/2,\beta}$ was about 4-fold lower, and the AUC_{inf} was only ~10% of that expected.

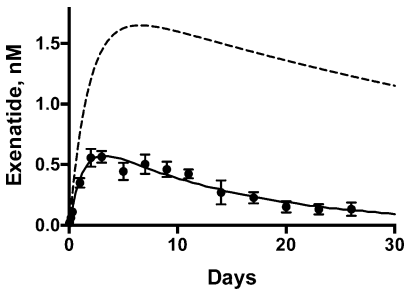

Figure 1. Pharmacokinetics of a hydrogel-L[CN]-exenatide conjugate containing 0.42 μmol exenatide in the rat. The solid line (-●-) shows serum exenatide in the rat from a SC hydrogel-exenatide showing an observed $t_{1/2,\beta}$ of 240 h and 10% of the expected AUC_{inf}; error bars show ± SEM. The dashed line (---) shows the expected C vs t for released exenatide assuming a $t_{1/2,\beta}$ of 1000 h.

DOI: 10.1021/acschembio.7b00218
ACS Chem. Biol. 2017, 12, 2107−2116

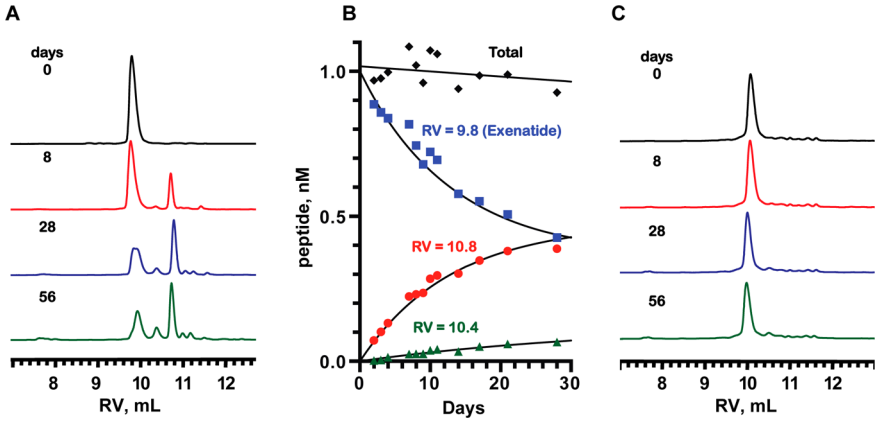

Figure 2. Exenatide and [Gln^{28}]exenatide stability in 200 mM NaP$_i$, pH 7.4, 37 °C. (A) HPLC traces at 0, 8, 28, and 56 days showing exenatide (top) converting to products (bottom). (B) Time course of exenatide (-■-, RV 9.8 mL) degradation ($t_{1/2}$ ∼ 10 days) and formation of new products with RV = 10.4 (-▲-; $t_{1/2}$ ∼ 5 wks) and 10.8 (-●-; $t_{1/2}$ ∼ 10 days) mL. The total peak area (-♦-) decreased ∼5% over 28 days. The rate of formation of the product at RV 9.9 could not be measured, and the two minor, latest-appearing peaks had $t_{1/2}$ ∼ 24 days (not shown). The reaction rates were estimated by plots of $\ln[1 - (C/C_{inf})]$ vs time for products and $\ln(C/C_{inf})$ vs time for loss of exenatide; C_{inf} values were estimated by optimizing the RMS of the linearity of such plots. (C) HPLC traces of [Gln^{28}]exenatide at 0 (top), 8, 28, and 56 (bottom) days. Peak areas were determined as a ratio of A_{280} to 200 μM of H-Lys(DNP)OH as an internal standard.

We considered the possibility that the low $t_{1/2,\beta}$ and AUC of the released exenatide were due to degradation of the peptide in the SC depot; if so, the measured serum exenatide would have underestimated the total released peptide. We note that degradation products in sera would not have been detected with the specific LC-MS/MS exenatide assay used. To estimate an *in vivo* rate of degradation, k_{deg}, of exenatide, eq 1 was transformed to eq 2 that describes the C vs t profile of exenatide with concomitant first-order degradation of the peptide bound to the depot.

$$[\text{Drug}]_{CC,t} = \text{Dose} \times \frac{F}{CL} k_1 (e^{(-k_1 + k_{deg})t} - e^{-k_a t}) \quad (2)$$

After the initial absorption phase, the slope of the log[Drug$_{CC}$] vs t plot becomes

$$k_\beta = k_1 + k_{deg} \quad (3)$$

and the difference between the observed and expected k_β values for drug release is k_{deg}. Using this approach, the observed vs expected curves in Figure 1 can be explained by a first-order destruction of the exenatide tethered to the hydrogel in the SC space with $t_{1/2,deg}$ ∼ 13 days.

Degradation of Exenatide. Modification of exenatide on the SC hydrogel could occur by proteolytic or chemical degradation. *A priori*, the former seemed more likely because exenatide is susceptible to enzymatic degradation,[31,32] and it seemed implausible that a spontaneous chemical degradation of exenatide would have gone unreported to date. Nevertheless, we examined the stability of exenatide under physiological conditions in the absence of enzymes.

We incubated exenatide in 200 mM NaP$_i$, pH 7.4, 37 °C, and analyzed samples at intervals by HPLC. As shown in Figure 2A, the exenatide peak disappeared as another developed at a similar retention volume (RV), and two slower eluting peaks emerged; two additional small peaks appeared at later times. At 56 days, the three major products had, in order of their RVs, estimated relative peak areas of ∼36, 12, and 46. Figure 2B shows the time-dependent changes of the peak areas of exenatide and two of the three major products. Taken together, these data show that exenatide is degraded with a $t_{1/2}$ of ∼10 days under the study conditions.

Product Identification. Exenatide has an AsnGly dipeptide in positions 28−29, a sequence that is particularly susceptible to Asn deamidation.[33−35] This well-studied reaction proceeds through formation of an unsymmetrical cyclic imide, which undergoes hydrolysis and isomerization to first give L-isoAsp and L-Asp, and later their D-isomers.

Exenatide: HGEGTFTSDLSKQMEEEAVRLFIEWLK-**N^{28}G**GPSSGAPPPS-NH$_2$

Following is evidence that Asn^{28} deamidation is the major source of exenatide degradation. First, as shown in Figure 2C and below, replacement of Asn^{28} by other amino acid residues prevented degradation, showing that other residues of exenatide are stable under the study conditions and localizing the degradation of exenatide to Asn^{28}. Second, each of the three major products showed $[M + H]^+$ = 4184.9 Da by ESI-MS, one mass unit higher than exenatide and consistent with the replacement of an amide NH$_2$ by an OH. The earliest eluting product peak (RV 9.9) coelutes with synthetic [L-Asp^{28}]-exenatide and is not a substrate for protein L-isoAsp methyltransferase (PIMT). The slow-eluting peak (RV 10.8 mL) is [L-isoAsp^{28}]exenatide since, as with deamidation of other AsnGly peptides, it is the largest peak and a substrate for PIMT. On the basis of relative formation rates in deamidation of other AsnGly peptides, and the absence of PIMT activity, the middle peak (RV 10.4) likely contains [D-isoAsp^{28}]exenatide. Taken together, these results conclusively show that Asn^{28} deamidation is the cause of *in vitro* degradation of exenatide.

When the mixture of degradation products (Figure 2A, t = 56 days) was tested in a cell-based GLP-1R assay in the agonist mode, it had a higher EC$_{50}$ than exenatide (Figure S2; Table S2); isolated [isoAsp^{28}] and synthetic [Asp^{28}]exenatides showed EC$_{50}$ values ∼2- to 4-fold higher than exenatide.

Deamidation of AsnGly in peptides is general-base catalyzed at near-neutral pH, with the rate dependent on buffer composition and concentration.[36] P$_i$ is a more effective catalyst than sulfonate, and at 20 mM sulfonate Asn deamidation rates are near the unbuffered rate. We examined deamidation rates of exenatide in 20 to 200 mM NaP$_i$ and HEPES buffers at pH 7.4

DOI: 10.1021/acschembio.7b00218
ACS Chem. Biol. 2017, 12, 2107−2116

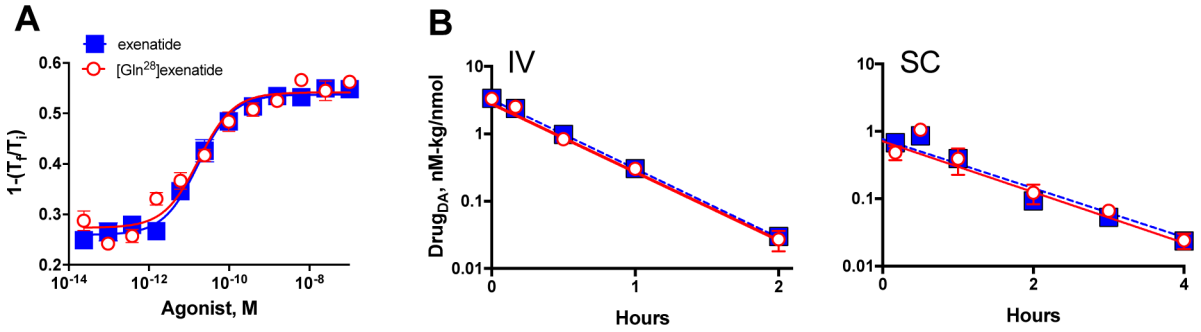

Figure 3. GLP-1RA activity and dose-adjusted C vs t plots of exenatide and [Gln^{28}]exenatide in the rat. (A) Comparison of exenatide (-■-) and [Gln^{28}]exenatide (-○-) in a cell-based hGLP-1R melanophore assay in agonist mode. T_i and T_f are initial and final response reads, respectively. EC_{50} exenatide = 17 pM, [Gln^{28}]exenatide = 17 pM. Points are averages ± SEM, and data were fit to a three-parameter logistic model (solid lines). (B) Dose-adjusted C vs t plots of serum peptides after IV (left panel) and SC (right panel) injections of 80 μg/kg exenatide (--■--) and 50 μg/kg of [Gln^{28}]exenatide (-○-) in the rat; dose adjustments made by dividing serum concentration by dose. Error bars are ± SEM (n = 3/group), which are not drawn if bars are shorter than the symbol. There were insufficient early time points to model distribution or absorption phases.

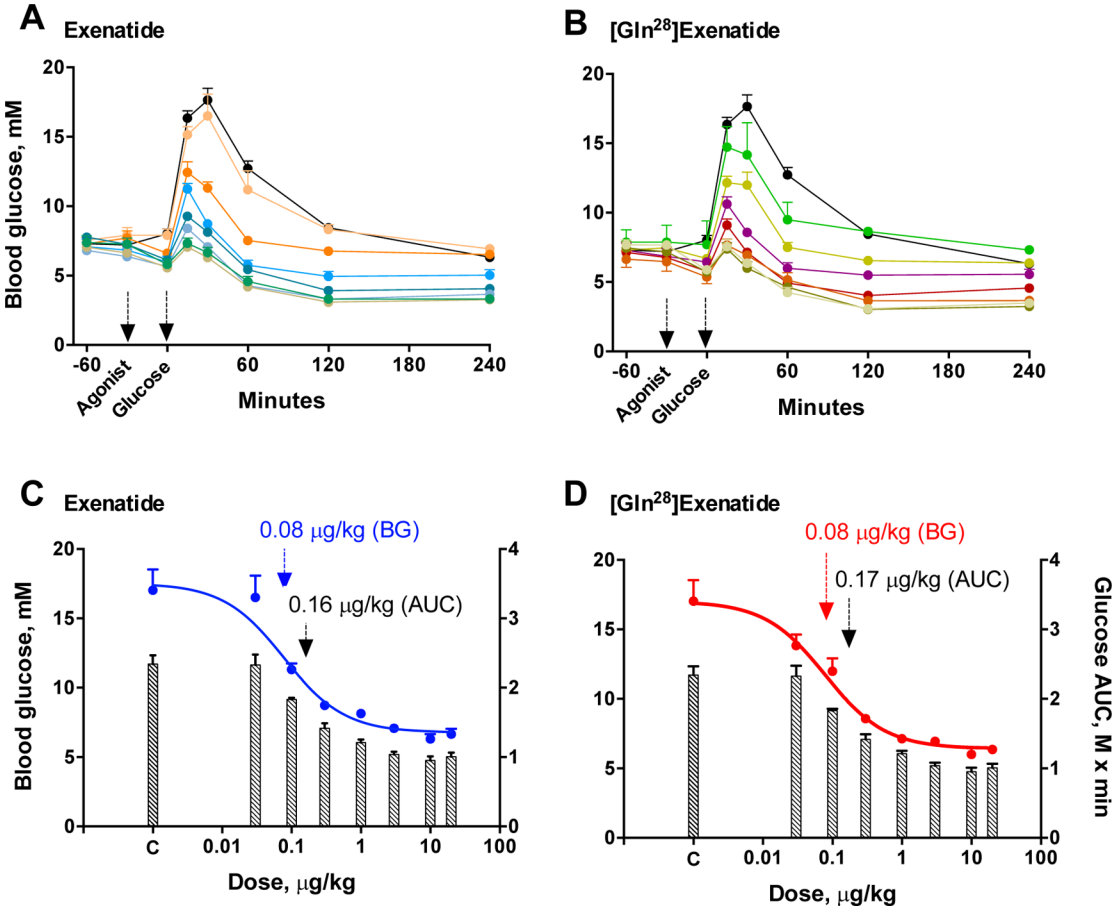

Figure 4. Acute glucose-lowering effects of exenatide and [Gln^{28}]exenatide in C57BL/6 mice. Blood glucose vs time after administration of (A) exenatide or (B) [Gln^{28}]exenatide 30 min prior to an OGTT; agonist doses are 0 (top), 0.03, 0.1, 0.3, 1, 3, 10, and 20 (bottom) μg/kg. Data from panels A and B are used to construct dose response curves (line) of blood glucose vs (C) exenatide dose, ED_{50}= 0.08 μg/kg, or (D) [Gln^{28}]exenatide, ED_{50}= 0.08 μg/kg, 30 min after glucose administration; bars show glucose AUC at 4 h after glucose administration for (C) exenatide, ED_{50} = 0.16 μg/kg, or (D) [Gln^{28}]exenatide, ED_{50}= 0.17 μg/kg. Values used for ED_{50} calculations were statistically different from those of the vehicle as shown by two-way RM ANOVA vs the vehicle, $p < 0.05$, Bonferroni post hoc test. Error bars show + SEM (n = 6 mice/group).

and 37 °C. At comparable concentrations, deamidation rates of exenatide were ∼2- to 4-fold faster in P_i than sulfonate; half-lives of deamidation ranged from 10 days in 200 mM P_i to 5 weeks in 20 mM HEPES.

Design of Stable Exenatide Analogs. We sought to modify the Asn^{28}Gly dipeptide of exenatide in a manner that would retain potent GLP-1R agonism but prevent deamidation. The latter can be accomplished by substituting either Asn or Gly by a number of amino acids that provide stable dipeptide sequences.[33] Our choice of which amino acid to substitute and what substitutions to make were influenced by the following considerations.

DOI: 10.1021/acschembio.7b00218
ACS Chem. Biol. 2017, 12, 2107−2116

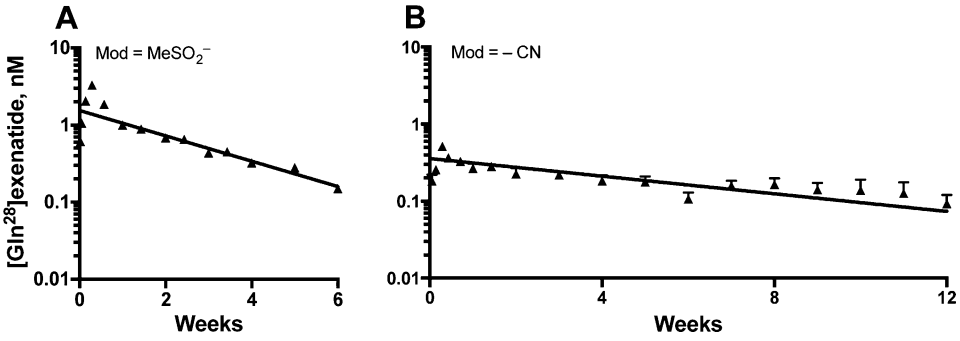

Figure 5. Serum [Gln^{28}]exenatide levels after SC injection of rats with microsphere conjugates. (A) After injection with [Gln^{28}]exenatide microspheres with a $MeSO_2$ modulator (0.17 μmol [Gln^{28}]exenatide/rat, 2.6 mg [Gln^{28}]exenatide/kg), $t_{1/2,\beta}$ was 310 h. (B) After injection with hydrogel-[Gln^{28}]exenatide microspheres with a −CN modulator (0.6 μmol [Gln^{28}]exenatide/rat, 8.9 mg [Gln^{28}]exenatide/kg), $t_{1/2,\beta}$ was 880 h. Early time points were insufficient to calculate absorption phase kinetics and were not used in fitting the β-phase shown. Error bars are + SEM (n = 6 rats/group). Analogous experiments in the mouse are provided in Figure S5.

In the 3-D structure of the exenatide-GLP-1R complex, the side chain of Asn^{28} is exposed to the solvent without contact to the receptor.[37] In contrast, Gly^{29} is in contact with GLP-1R and has a rare +97° ϕ dihedral angle. We avoided changing Gly^{29} because a change might perturb important interactions with the receptor and/or the peptide backbone conformation and because it—but not Asn^{28}—is a known epitope for exenatide-induced antibodies in humans.[38]

We chose Gln as a substitute for Asn^{28} because of its high structural similarity and being less prone toward deamidation.[33] We also chose Ala, Asp, and Lys modifications since they are the most frequent substitutions for Asn at structurally equivalent positions in related proteins.[39]

We prepared the Ala, Asp, Gln, and Lys substitutions for Asn^{28} of exenatide by SPPS. All [Xaa^{28}]exenatides had EC_{50} values (17- to 41 pM) comparable to exenatide (17 pM) in a GLP-1RA assay (Figure S1). Upon extended incubation (~3 months) of these [Xaa^{28}]exenatides in 200 mM P_i, at pH 7.4 and 37 °C, major new peaks were not observed, except for [Asp^{28}]exenatide, which slowly isomerized to [isoAsp^{28}]-exenatide.[34] At low peptide concentrations (~0.2 mM), we observed small losses in A_{280} consistent with nonspecific adsorption to vessel surfaces.[40] At 2 mM [Gln^{28}]exenatide, we estimated that the $t_{1/2}$ for loss of peptide was 30 weeks. Hence, [Gln^{28}]exenatide is very stable under physiological conditions.

GLP-1R Activation, Pharmacokinetics, and Glucoregulatory Effects of [Gln^{28}]exenatide. We chose [Gln^{28}]-exenatide for further study because its high structural similarity to exenatide suggested it is most likely to be similar in pharmacokinetic and pharmacodynamic properties, and least likely to have off-target effects or generate additional antibodies; the additional $-CH_2-$ group only represents a 0.3% increase in MW over exenatide.

Figure 3 shows that exenatide and [Gln^{28}]exenatide have identical agonist activity in a cell-based GLP-1R assay. Further, the EC_{50} of [Gln^{28}]exenatide was unchanged after 8 weeks, demonstrating its stability as an agonist.

We compared the pharmacokinetics of [Gln^{28}]exenatide and exenatide in the rat and mouse. Whether administered IV or SC, the dose-adjusted pharmacokinetics of [Gln^{28}]exenatide and exenatide in the rat are indistinguishable (Figure 3B; Table S3). As reported for exenatide,[30] the data for SC administration of both peptides are consistent with a flip-flop mechanism with rate-determining absorption having a $t_{1/2}$ of 50 min, followed by an elimination phase with $t_{1/2}$ of 18 min. The dose adjusted AUCs for IV and SC exenatide and [Gln^{28}]exenatide gave SC bioavailabilities of 62−69% (Table S3), comparing well to 65−75% reported for exenatide.[30] In the mouse, we obtained $t_{1/2,\beta}$ of 20 min for SC injection identical to that reported for exenatide (Figure S4). Thus, the pharmacokinetic parameters of [Gln^{28}]exenatide and exenatide in rodents were indistinguishable.

We next compared the acute glucoregulatory effects of [Gln^{28}]exenatide and exenatide in the mouse. The peptides were administered as single SC injections to nondiabetic C57BL/6 mice 30 min prior to an oral glucose tolerance test (OGTT), and blood glucose and insulin were measured over the subsequent 6 h (Figure 4A,B). Increasing amounts of either [Gln^{28}]exenatide or exenatide caused nearly identical decreases in glucose excursions. The glucose lowering after 30 min by [Gln^{28}]exenatide was identical to that for exenatide (ED_{50} = 0.08 μg/kg; Figure 4C). Likewise, the dose-dependent decrease of AUC for blood glucose over the study period for [Gln^{28}]exenatide and exenatide were the same (Figure 4D). Finally, there was a rise in insulin 15 min after the glucose load that peaked at ~0.3 to 1 μg/kg [Gln^{28}]exenatide or exenatide and then decreased with higher concentrations to give a bell-shaped curve as reported for exenatide[41,42] (Figure S6). Thus, the acute glucoregulatory and insulinotropic effects of [Gln^{28}]-exenatide and exenatide were identical.

Hydrogels with Releasable [Gln^{28}]exenatide. [Gln^{28}]-exenatide microspheres were prepared as described for analogous exenatide conjugates.[28] Accelerated release studies of conjugates with $MeSO_2$ and −CN modulators in the linkers gave estimated $t_{1/2}$ values of 620 and 1980 h, respectively, at pH 7.4 and 37 °C. The cross-links of these microspheres also contained self-cleaving linkers tuned to degrade the polymer after drug release.[43]

Microspheres were injected SC into normal rats, and [Gln^{28}]exenatide in serum was measured by LC-MS/MS (Figure 5). The hydrogel using the $MeSO_2$ modulator showed a $t_{1/2,\beta}$ of 13 days, and that with the −CN modulator showed a $t_{1/2,\beta}$ of 37 days, some 1.5- to 3.7-fold longer than corresponding exenatide conjugates (Figure 1 and ref 28). A pharmacokinetic study of these microspheres in the mouse gave slightly shorter $t_{1/2,\beta}$ values of serum [Gln^{28}]exenatide of 10 and 30 days for the $MeSO_2$ and −CN modulators, respectively (Figure S5, Table S4). The 95% confidence levels for the $t_{1/2,\beta}$ values of the −CN linker in the mouse (24.6 to 40.5 days) and rat (27.4 to 56.2 days) are extensively overlapping, as are those

DOI: 10.1021/acschembio.7b00218
ACS Chem. Biol. 2017, 12, 2107−2116

for the $MeSO_2$ linker (7.7 to 15.1 days in mouse vs 11.1 to 15.6 days in rat). In the absence of strong statistical evidence for difference, we use the $t_{1/2,\beta}$ of the linkers in the rat in the ensuing analyses and discussion.

If we assume the pharmacokinetics of the hydrogel-exenatide and [Gln^{28}]exenatide conjugates differ only because of the deamidation of the former, we can estimate the rate of *in vivo* deamidation, k_{deg}, using eq 1 to obtain k_1 for [Gln^{28}]exenatide, eq 2 to obtain $k_1 + k_{deg}$ for exenatide and then solving for k_{deg} in eq 3. From this, we estimate the *in vivo* $t_{1/2}$ values of deamidation of exenatide in the rat as 14 days for either linker. This value is in excellent accord with the estimated $t_{1/2,deg}$ for exenatide deamidation of ∼13 days from the simulated expected and experimentally observed $t_{1/2,\beta}$ values of the hydrogel-exenatide conjugate obtained at the outset of this study (Figure 1).

Eight-Week Pharmacodynamic Effects of Once-Monthly Administered [Gln^{28}]exenatide Microspheres. The male Zucker diabetic fatty (ZDF) rat—a widely used model for obese T2D in humans[44]—develops diabetes between 6 and 10 weeks of age when fed a high fat diet and undergoes a progressive deterioration of beta-cell function in the face of insulin resistance. After the onset of disease, they show signs of T2D such as hyperglycemia, insulin resistance, increased food and water intake, weight gain, and increased gastric emptying rate; they also show diminished glucose lowering and insulin responses when challenged with glucose in an OGTT, and increased HbA1c after prolonged hyperglycemia. Continuous exposure to GLP-1RAs improves most of these diabetic pathological changes.[1,45]

We compared the 8-week pharmacodynamic effects of the long-acting releasable microsphere−[Gln^{28}]exenatide (Mod=−CN) with continuously infused exenatide (CI-exenatide) in 8 week old male ZDF rats. Eligible rats were stratified into four groups (10/group) based on morning fed blood glucose and individual groups received: (a) Alzet pump vehicle control (50 mM NaOAc, pH 4.5); (b) Alzet pump with 0.2 μg/mL exenatide in vehicle delivered at 30 μg/kg/day; QM injections of SC microsphere−[Gln^{28}]exenatide at (c) 920 μg and (d) 9200 μg/kg along with vehicle control pumps. The dose of CI-exenatide and the lower dose of [Gln^{28}]exenatide microspheres were both targeted to give a C_{min} of ∼0.1 nM serum peptide and the higher dose of [Gln^{28}]exenatide microspheres, at a C_{min} of 1 nM. After four weeks, pumps were replaced, and rats were reinjected with [Gln^{28}]exenatide microspheres at the same doses.

All studied pharmacodynamic effects of two monthly SC injections of 920 μg/kg microsphere−[Gln^{28}]exenatide closely tracked those of 30 μg/kg/day CI-exenatide (Table 1, Figures 6 and S7); expectedly, the 10-fold higher dose of [Gln^{28}]-exenatide microspheres showed more pronounced antidiabetic effects. Analyses of serum peptides at eight weekly intervals gave *C* vs *t* plots very close to what was anticipated (Figure S8); the data showed a C_{ave} of 0.13 and 1.2 nM for the low and high doses of microsphere−[Gln^{28}]exenatide, respectively, and 0.17 pM for exenatide CI.

Animals treated with CI-exenatide and microsphere-[Gln^{28}]-exenatide showed a rapid decrease in blood glucose that persisted over the 8-week study period albeit with a slow, consistent rise as the ZDF rats became more diabetic (Figure 6A; Table 1). The glucose-lowering effects translated into significant reduction of HbA1c levels—a measure of cumulative blood glucose levels—compared to untreated animals on days 26 and 55 (Figure 6B); notably, the higher dose of [Gln^{28}]exenatide microspheres actually decreased HbA1c levels below pretreatment levels. Both CI-exenatide and [Gln^{28}]-exenatide microspheres reduced food and water intake over the entire study period in a manner characteristic of continuous exposure of ZDF rats to GLP-1RAs[45,46] (Table 1, Figure S7). Initially, treated animals showed a rapid weight loss; after ∼3 days, weight gain increased, and after ∼4 weeks the weights of treated rats exceeded that of controls (Figure S7). Despite hyperphagia, body weight gain of severely diabetic ZDF rats is impacted by a significant loss of calories via glucosuria;[44] ZDF rats treated with a long-acting GLP-1RA show improved diabetes and may not suffer this caloric loss, resulting in paradoxical weight gain despite lower food intake.[45]

Table 1. Relative Cumulative Food and Water Intake and Average Blood Glucose over the 8 Week Study Period in the ZDF Rat[a]

	vehicle	CI-exenatide (30 μg/kg/day)	MS-[Gln^{28}]Ex (920 μg/kg)	MS-[Gln^{28}]Ex (9200 μg/kg)
food intake	100 ± 2	74 ± 4	68 ± 4	55 ± 2
water intake	100 ± 6	51 ± 9	42 ± 8	25 ± 1
blood glucose	100 ± 2	64 ± 8	57 ± 9	40 ± 2

[a]The values of serial data of treated animals (Figure S7) were determined over 8 weeks and are expressed as the percent of that observed in the vehicle control.

In the OGTT performed on days 26 and 55, treated animals showed significantly improved glucose responses and AUC values, together with a greater insulin secretory response (Figures 6C,D, S7). The robust antihyperglycemic and insulinotropic effects of the [Gln^{28}]exenatide microspheres persist throughout the eight-week treatment period and indicate preservation of beta cells. Last, there was no difference between treated and untreated rats in gastric emptying rate (Figure S7), in accord with the desensitization of acute inhibition that is observed after continuous exposure to GLP-1RAs.[47]

After the study period, pumps were removed and animals were maintained for four additional weeks. Because of the short $t_{1/2,\beta}$ of exenatide, glucose levels, as well as food and water intake of rats withdrawn from CI-exenatide rapidly reverted to control levels (Figures 6A, S7). Rats treated with [Gln^{28}]-exenatide microspheres reverted more slowly since the drug-releasing depot remained in the animals. HbA1c levels at day 85 likewise reflected the rapid reversion of animals treated with CI-exenatide, and slower reversion of rats treated with extended-release [Gln^{28}]exenatide microspheres.

In summary, the above results convincingly demonstrate that in the diabetic ZDF rat model of T2D, the chronic pharmacodynamic effects of once-monthly injected [Gln^{28}]-exenatide microspheres are dose dependent and indistinguishable from those observed with continuous exposure to native exenatide.

Pharmacokinetic Simulations in the Human. We previously described an approach for interspecies modeling of the pharmacokinetics of drugs released from β-eliminative linkers attached to noncirculating carriers.[28] The simulation requires knowledge of the linker cleavage rate, which, although not yet determined in humans, is chemically controlled and apparently species-independent.[25,48] Notably, the serum $t_{1/2,\beta}$

DOI: 10.1021/acschembio.7b00218
ACS Chem. Biol. 2017, 12, 2107−2116

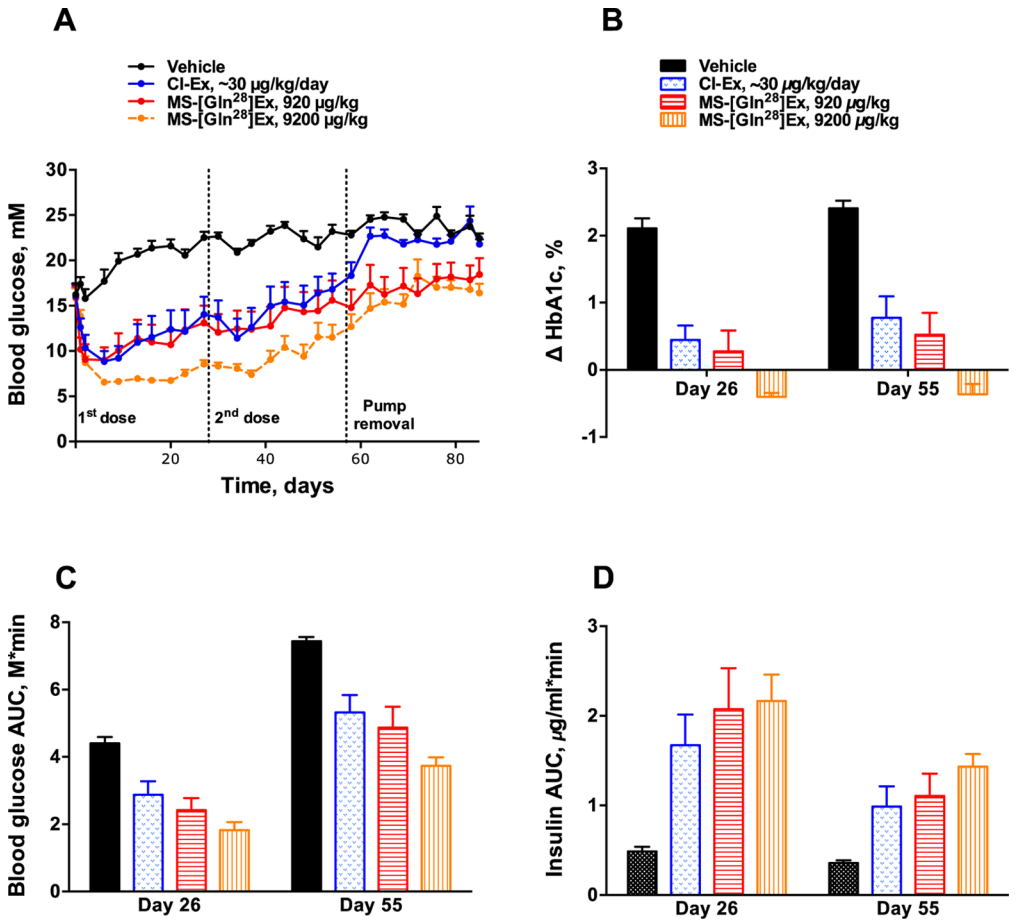

Figure 6. Effects of two monthly SC injections of [Gln^{28}]exenatide microspheres vs CI-exenatide on glucose homeostasis in diabetic male ZDF rats. Effects on (A) blood glucose levels (morning fed glucose) and (B) HbA1c levels at days 26 and 55. At days 26 and 55, OGTTs were performed measuring (C) blood glucose and (D) insulin AUC values. Bar graph columns represent vehicle control (solid), 30 μg/kg/day CI-exenatide (dotted), 920 μg/kg (horizontal lines) and 9200 μg/kg (vertical lines) [Gln^{28}]exenatide microspheres. Data show mean + SEM (n = 10 mice/group). Data analyzed by one-way ANOVA (bar graphs) or two-way repeated measures ANOVA (line graphs) with Bonferroni posthoc test. *p < 0.05, **p < 0.01, ***p < 0.001.

Table 2. Reported and Simulated Steady State Pharmacokinetic Parameters of Exenatide and [Gln^{28}]exenatide Released from Delivery Systems in Humans

		serum exenatide or [Gln^{28}]exenatide					
drug (modulator)	dosing interval	dose, mg/mo (wk)[a]	$t_{1/2,\beta}$, h	C_{min}, nM	C_{max}, nM	C_{max}/C_{min}	AUC nM-h/wk
Bydureon[b]	QW	8 (2)	NA	0.07	0.12	1.7[c]	57
CI-exenatide (ITCA 650)		1.7 (0.42)	NA	0.07	0.07	1.0	12
MS-exenatide ($MeSO_2$-)	QM	10.4[d]	160	0.07	1.31	18.7	74
MS-exenatide (−CN)	QM	5.4[d]	240	0.07	0.51	7.2	38
MS-[Gln^{28}]exenatide ($MeSO_2$-)	QM	4.2[d]	310	0.07	0.33	4.7	29
MS-[Gln^{28}]exenatide (−CN)	QM	2.6[d]	880	0.07	0.13	1.8	16

[a]One month is assumed to have 28 days. [b]Bydureon PK parameters from refs 50 and 51. [c]Four excursions per month. [d]Dose values for simulations assume 100% bioavailability of [Gln^{28}]exenatide and exenatide in the human, as it is with SC exenatide (Byetta label).

values of [Gln^{28}]exenatide released from the two microsphere conjugates studied here are, within experimental error, the same in the mouse and rat.

Eq 4 describes the steady state dose needed to maintain the drug concentration above a therapeutic minimum concentration C_{min} for a specified interval, t_{min}.[28]

$$\text{Dose}_{ss} = C_{min}\frac{CL}{Fk_1}(e^{k_1 t_{min}} - 1) \quad (4)$$

For dosage estimations in humans, we calculated the CL of exenatide as 0.123 L/h/kg from CL = $\text{Dose}_{SS}/C_{SS}/BW$ using the results of 25 ng/min CI-exenatide.[49] From this, and the V_d of 0.4 L/kg and F = 1 (Byetta package), we estimated an elimination $t_{1/2,\beta}$ of 2.3 h, in excellent agreement with the 2.4 h $t_{1/2,\beta}$ for SC injection (Byetta label). Although analogous values for [Gln^{28}]exenatide in humans are not known, we justify using those of exenatide because of the high structural similarity and the near-identical GLP-1R EC_{50} values, pharmacokinetics, and *in vivo* glucoregulatory effects in rodents. We targeted the

DOI: 10.1021/acschembio.7b00218
ACS Chem. Biol. 2017, 12, 2107−2116

exenatide therapeutic C_{min} of ~70 pM that is achieved with a 2 mg weekly dose Bydureon,[50,51] calculated the dose from eq 4, and estimated the C_{max} and steady state AUC from superposition of single dose C vs t plots (eq 1).

Simulated steady state parameters of drug released from hydrogel-exenatide and [Gln^{28}]exenatide conjugates are compared in Table 2. QW Bydureon serves as a comparator, and its reported C_{max} and C_{max}/C_{min} values serve as guidance for limits known to be tolerable. We also show values for continuous infusion of 60 μg/day exenatide via the Medici implantable pump drug delivery system that achieves a constant ~70 pM concentration and represents the lowest efficacious dose and the most efficient AUC that maintains the therapeutic C_{min}.[24] Higher AUC values of other delivery systems represent "wasted" exposure.

The previously reported QW exenatide conjugate $t_{1/2,\beta}$ of ~7 days for released exenatide[28] would require a high dose to span the four half-lives needed to support QM administration and have unacceptably high C_{max} and C_{max}/C_{min} values compared to Bydureon. With the CN modulator, the $t_{1/2,\beta}$ of released exenatide increases to 240 h, but with an estimated deamidation $t_{1/2}$ of ~14 days (Figure 1) is unsuitable for QM dosing.

[Gln^{28}]exenatide microspheres with a $MeSO_2$ modulator has a $t_{1/2,\beta}$ for the released peptide that would be suitable for biweekly administration, but not for QM administration because the C_{max}/C_{min} would be ~3-fold higher than weekly Bydureon. With the −CN modulator and [Gln^{28}]exenatide, the $t_{1/2,\beta}$ is a very long 37 days and should maintain the drug serum levels $\geq C_{min}$ with only ~2.6 mg of peptide/month, while maintaining a C_{max} and C_{max}/C_{min} that is similar to that for each QW Bydureon dose. As measured by the AUC, the efficiency of drug utilization was 75% of the near-perfect CI-exenatide. It would take ~12 weeks for the [Gln^{28}]exenatide to reach steady state, which is not much longer than the 8 to 10 weeks needed for QW Bydureon. However, by administering a loading dose twice the steady state dose, and initiating monthly injections at week 3, the steady state C_{min} would be reached by day 2 and the steady state C_{max} would never be exceeded. We note that this conjugate would require a monthly injection of less than 0.5 mL of microspheres which contains ~4 mg of exenatide.

DISCUSSION

The primary objective of this work was to develop a long-acting GLP-1RA that could be administered by monthly SC injections. Compared to current QW agonists, obvious benefits would be greater patient convenience, compliance, and persistence. A longer-acting agonist would also allow advancing or delaying a dose for a short period and lessen the burden of caregivers responsible for drug administration to reliant patients. Therapeutic benefits could as well be realized after QM GLP-1RAs are validated and have undergone appropriate clinical studies.

The approach we used was to tether a GLP-1RA to a hydrogel microsphere depot by a self-cleaving β-eliminative linker with a preprogrammed cleavage rate; upon subcutaneous injection, the linker slowly cleaves and releases the drug into the systemic circulation. We previously used this approach to prepare a hydrogel-exenatide conjugate that should support weekly administration in the human.[28]

In preliminary work, we attempted to increase the duration of exenatide exposure by using a slower-cleaving linker but found a less than expected $t_{1/2,\beta}$ and exposure. We speculated that the unexpected pharmacokinetic result was due to degradation of the hydrogel-bound peptide, and found that exenatide undergoes spontaneous deamidation at Asn^{28}, which we estimated would have a half-life of ~14 days *in vivo*. The deamidation products—Asp and isoAsp-containing peptides—are agonists of the GLP-1R but were not detectable in the assays used for serum exenatide. Although it is possible these products would not greatly affect the pharmacological activity, we elected to avoid degradation products rather than study them. Parenthetically, a similar deamidation of Asn^{28} is likely to occur in other long-acting GLP-1 agonists that have exenatide-related sequences containing an AsnGly dipeptide.[22,52]

We subsequently showed that substitution of Asn^{28} by several other amino acid residues stabilizes the peptide while maintaining excellent agonist activity for hGLP-1R. We selected [Gln^{28}]exenatide for further study because its close structural similarity to exenatide—a single methylene group difference—suggested it should be most analogous in pharmacokinetic and pharmacodynamic properties and least likely to generate off-target effects or additional antibodies. We showed that [Gln^{28}]exenatide has identical GLP-1RA activity, pharmacokinetics, and glucoregulatory effects to native exenatide but does not suffer the instability of the parent peptide.

We attached [Gln^{28}]exenatide to hydrogel microspheres *via* two different β-eliminative linkers previously used in analogous exenatide conjugates, injected the microspheres SC in the mouse and the rat, and measured serum [Gln^{28}]exenatide over time. Pharmacokinetic analyses showed serum half-lives of about 2 weeks and one month for the released [Gln^{28}]-exenatide. Two monthly administrations of the longer-acting [Gln^{28}]exenatide microspheres in the rat showed identical pharmacodynamic effects as continuously infused exenatide over the same period.

Pharmacokinetic simulations indicated that the conjugate with a $t_{1/2,\beta}$ of about one month would favorably support once-monthly administration in humans. It should maintain a continuous therapeutic serum concentration with monthly C_{max} and C_{max}/C_{min} values comparable to or lower than those of currently available QW GLP-1 agonists. The QM [Gln^{28}]-exenatide-microsphere formulation has other desirable features: (a) It can be injected SC in a small volume through a small bore 27- to 30-gauge needle. (b) It can be stored for long periods as a slightly acidic liquid suspension of microspheres amenable for use in a prefilled autoinjection device. (c) It does not require reconstitution of components before self-administration. (d) Significantly reduced costs should be realized since the delivery system requires less frequent dosing than current formulations.

In summary, we have developed a novel drug delivery system for a peptidic GLP-1RA that is a viable candidate for once-monthly SC administration for treatment of type 2 diabetes. The [Gln^{28}]exenatide microspheres could provide a new option for T2D patients that desire a longer dosing interval than current QW formulations but are reluctant to have an osmotic pump surgically implanted that can deliver a GLP-1RA over a longer duration.

MATERIALS AND METHODS

The source of specialized materials is provided along with their use in the Supporting Information. Detailed synthetic, conjugation, and analytical procedures are described. *In vitro* kinetic procedures are provided as are *in vivo* pharmacokinetic and pharmacodynamics methods and analyses.

DOI: 10.1021/acschembio.7b00218
ACS Chem. Biol. 2017, 12, 2107−2116

■ ASSOCIATED CONTENT

Supporting Information

The Supporting Information is available free of charge on the ACS Publications website at DOI: 10.1021/acschembio.7b00218.

Materials and Methods, (Figure S1) hGLP-1R assays of [Xaa^{28}]exenatides, (Figure S2) GLP-1R bioassays of exenatide and its degradation products, (Figure S3) isoAsp determinations in exenatide degradation, (Figure S4) C vs t of serum exenatide and [Gln^{28}]exenatide in mice, (Figure S5) serum [Gln^{28}]exenatide after SC injection of mice with microsphere conjugates, (Figure S6) insulin levels of varying doses of exenatide and [Gln^{28}]exenatide in OGTTs, (Figure S7) three month pharmacodynamic study in ZDF rats, (Figure S8) GLP-1RAs serum levels in ZDF rats, (Table S1) EC_{50} values of synthetic [Xaa^{28}]exenatide in GLP-1R assays, (Table S2) EC_{50} of [Asp^{28}]exenatide and exenatide deamidation products, (Table S3) pharmacokinetic parameters of exenatide and [Gln^{28}]exenatide in the rat, (Table S4) pharmacokinetic properties of [Gln^{28}]exenatide microspheres (PDF)

■ AUTHOR INFORMATION

Corresponding Author

*Phone 415 552 5306. E-mail: Daniel.V.Santi@prolynxllc.com.

ORCID

Eric L. Schneider: 0000-0001-7274-7961

Daniel V. Santi: 0000-0002-3790-0673

Author Contributions

E.L.S, B.R.H., S.J.P., R.R., N.V., and G.W.A. designed and performed experiments and analyzed data. D.G.P. and D.V.S. provided methodological and conceptual input, and D.V.S. wrote the manuscript.

Notes

The authors declare the following competing financial interest(s): E.L.S, B.R.H., S.J.P., R.R., N.V., G.W.A., D.G.P., and D.V.S. hold options or stock in the company.

■ ACKNOWLEDGMENTS

We thank H. Jo and W. Degrado for preparing peptides, M. Mebrahtu for performing the melanophore bioassays, and A. Sali for assistance with structural features of the exenatide-GLP-1R interaction. This work was supported in part by NSF grant 1429972.

■ REFERENCES

(1) Madsbad, S. (2016) Review of head-to-head comparisons of glucagon-like peptide-1 receptor agonists. *Diabetes, Obes. Metab. 18*, 317−332.

(2) Campbell, J. E., and Drucker, D. J. (2013) Pharmacology, physiology, and mechanisms of incretin hormone action. *Cell Metab. 17*, 819−837.

(3) Hanna, A., Connelly, K. A., Josse, R. G., and McIntyre, R. S. (2015) The non-glycemic effects of incretin therapies on cardiovascular outcomes, cognitive function and bone health. *Expert Rev. Endocrinol. Metab. 10*, 101−114.

(4) Madsbad, S. (2014) The role of glucagon-like peptide-1 impairment in obesity and potential therapeutic implications. *Diabetes, Obes. Metab. 16*, 9−21.

(5) Potts, J. E., Gray, L. J., Brady, E. M., Khunti, K., Davies, M. J., and Bodicoat, D. H. (2015) The Effect of Glucagon-Like Peptide 1 Receptor Agonists on Weight Loss in Type 2 Diabetes: A Systematic Review and Mixed Treatment Comparison Meta-Analysis. *PLoS One 10*, e0126769.

(6) Baggio, L. L., and Drucker, D. J. (2014) Glucagon-like peptide-1 receptors in the brain: controlling food intake and body weight. *J. Clin. Invest. 124*, 4223−4226.

(7) Marso, S. P., Daniels, G. H., Brown-Frandsen, K., Kristensen, P., Mann, J. F., Nauck, M. A., Nissen, S. E., Pocock, S., Poulter, N. R., Ravn, L. S., Steinberg, W. M., Stockner, M., Zinman, B., Bergenstal, R. M., and Buse, J. B. (2016) Liraglutide and Cardiovascular Outcomes in Type 2 Diabetes. *N. Engl. J. Med. 375*, 311.

(8) Marso, S. P., Bain, S. C., Consoli, A., Eliaschewitz, F. G., Jodar, E., Leiter, L. A., Lingvay, I., Rosenstock, J., Seufert, J., Warren, M. L., Woo, V., Hansen, O., Holst, A. G., Pettersson, J., and Vilsboll, T. (2016) Semaglutide and Cardiovascular Outcomes in Patients with Type 2 Diabetes. *N. Engl. J. Med. 375*, 1834.

(9) Ussher, J. R., and Drucker, D. J. (2014) Cardiovascular actions of incretin-based therapies. *Circ. Res. 114*, 1788−1803.

(10) Drucker, D. J. (2016) The Cardiovascular Biology of Glucagon-like Peptide-1. *Cell Metab. 24*, 15−30.

(11) Armstrong, M. J., Gaunt, P., Aithal, G. P., Barton, D., Hull, D., Parker, R., Hazlehurst, J. M., Guo, K., Abouda, G., Aldersley, M. A., Stocken, D., Gough, S. C., Tomlinson, J. W., Brown, R. M., Hubscher, S. G., and Newsome, P. N. (2016) Liraglutide safety and efficacy in patients with non-alcoholic steatohepatitis (LEAN): a multicentre, double-blind, randomised, placebo-controlled phase 2 study. *Lancet 387*, 679−690.

(12) Parkes, D. G., Mace, K. F., and Trautmann, M. E. (2013) Discovery and development of exenatide: the first antidiabetic agent to leverage the multiple benefits of the incretin hormone, GLP-1. *Expert Opin. Drug Discovery 8*, 219−244.

(13) Tibble, C. A., Cavaiola, T. S., and Henry, R. R. (2013) Longer Acting GLP-1 Receptor Agonists and the Potential for Improved Cardiovascular Outcomes. *Expert Rev. Endocrinol. Metab. 8*, 247−259.

(14) Polonsky, W. H., and Henry, R. R. (2016) Poor medication adherence in type 2 diabetes: recognizing the scope of the problem and its key contributors. *Patient Prefer. Adherence 10*, 1299−1307.

(15) Freemantle, N., Satram-Hoang, S., Tang, E. T., Kaur, P., Macarios, D., Siddhanti, S., Borenstein, J., and Kendler, D. L. (2012) Final results of the DAPS (Denosumab Adherence Preference Satisfaction) study: a 24-month, randomized, crossover comparison with alendronate in postmenopausal women. *Osteoporosis Int. 23*, 317−326.

(16) Tkacz, J., Ellis, L., Bolge, S. C., Meyer, R., Brady, B. L., and Ruetsch, C. (2014) Utilization and adherence patterns of subcutaneously administered anti-tumor necrosis factor treatment among rheumatoid arthritis patients. *Clin. Ther. 36*, 737−747.

(17) Kishimoto, H., and Maehara, M. (2015) Compliance and persistence with daily, weekly, and monthly bisphosphonates for osteoporosis in Japan: analysis of data from the CISA. *Arch. Osteoporos 10*, 231.

(18) Zierhut, M. L., and Cirincione, B. B. (2014) Method for treating diabetes with extended release formulation of GLP-1 receptor agonists, US 2014/0220134 A1.

(19) Wysham, C. H., MacConell, L., and Hardy, E. (2016) Efficacy and Safety of Multiple Doses of Exenatide Once-Monthly Suspension in Patients With Type 2 Diabetes: A Phase 2 Randomized Clinical Trial. *Diabetes Care 39*, 1768.

(20) Del Prato, S., Kang, J., Choi, S., Lee, W., Han, O., Kil, S., Gee, K., Choi, I. Y., Kwon, S. C., Trautmann, M., and Hompesch, M. (2015) Once-a-Month Treatment with HM11260C Improves Glycemic Control in Type 2 Diabetes (T2DM)—Interim Data from a 16-Week Study. In *American Diabetes Association (ADA) 75th Scientific Sessions*, June 5−9, 2015, Boston, Massachusetts; Abstract 105-LB.

(21) Rosenstock, J., Reusch, J., Bush, M., Yang, F., and Stewart, M. (2009) Potential of albiglutide, a long-acting GLP-1 receptor agonist, in type 2 diabetes: a randomized controlled trial exploring weekly, biweekly, and monthly dosing. *Diabetes Care 32*, 1880−1886.

(22) Podust, V. N., Balan, S., Sim, B. C., Coyle, M. P., Ernst, U., Peters, R. T., and Schellenberger, V. (2015) Extension of in vivo half-life of biologically active molecules by XTEN protein polymers. *J. Controlled Release 240*, 52.
(23) Cleland, J., Aronson, R., Humphriss, E., Shore, C. R., Bright, G., Zhou, R., and Kipnes, M. S. (2012) Safety, pharmacokinetics, and pharmacodynamics of a single subcutaneous dose of VRS-859 in patients with type 2 diabetes. In *European Association for the Study of Diabetes (EASD) 48th Annual Meeting*, Abstract #821, S338−S339, Diabetologia, Berlin, Germany.
(24) Henry, R. R., Rosenstock, J., Logan, D., Alessi, T., Luskey, K., and Baron, M. A. (2014) Continuous subcutaneous delivery of exenatide via ITCA 650 leads to sustained glycemic control and weight loss for 48 weeks in metformin-treated subjects with type 2 diabetes. *J. Diabetes Complications 28*, 393−398.
(25) Santi, D. V., Schneider, E. L., Reid, R., Robinson, L., and Ashley, G. W. (2012) Predictable and tunable half-life extension of therapeutic agents by controlled chemical release from macromolecular conjugates. *Proc. Natl. Acad. Sci. U. S. A. 109*, 6211−6216.
(26) Ashley, G. W., Henise, J., Reid, R., and Santi, D. V. (2013) Hydrogel drug delivery system with predictable and tunable drug release and degradation rates. *Proc. Natl. Acad. Sci. U. S. A. 110*, 2318−2323.
(27) Henise, J., Hearn, B. R., Ashley, G. W., and Santi, D. V. (2015) Biodegradable tetra-PEG hydrogels as carriers for a releasable drug delivery system. *Bioconjugate Chem. 26*, 270−278.
(28) Schneider, E. L., Henise, J., Reid, R., Ashley, G. W., and Santi, D. V. (2016) Hydrogel Drug Delivery System Using Self-Cleaving Covalent Linkers for Once-a-Week Administration of Exenatide. *Bioconjugate Chem. 27*, 1210−1215.
(29) Schneider, E. L., Hearn, B. R., Pfaff, S. J., Fontaine, S. D., Reid, R., Ashley, G. W., Grabulovski, S., Strassberger, V., Vogt, L., Jung, T., and Santi, D. V. (2016) Approach for Half-Life Extension of Small Antibody Fragments That Does Not Affect Tissue Uptake. *Bioconjugate Chem. 27*, 2534.
(30) Parkes, D., Jodka, C., Smith, P., Nayak, S., Rinehart, L., Gingerich, R., Chen, K., and Young, A. (2001) Pharmacokinetic Actions of Exendin-4 in the Rat: Comparison With Glucagon-Like Peptide-1. *Drug Dev. Res. 53*, 260−267.
(31) Chen, J., Yu, L., Wang, L., Fang, X., Li, L., and Li, W. (2007) Stability of synthetic exendin-4 in human plasma in vitro. *Protein Pept. Lett. 14*, 19−25.
(32) Liao, S., Liang, Y., Zhang, Z., Li, J., Wang, J., Wang, X., Dou, G., Zhang, Z., and Liu, K. (2015) In vitro metabolic stability of exendin-4: pharmacokinetics and identification of cleavage products. *PLoS One 10*, e0116805.
(33) Robinson, N. E., Robinson, Z. W., Robinson, B. R., Robinson, A. L., Robinson, J. A., Robinson, M. L., and Robinson, A. B. (2004) Structure-dependent nonenzymatic deamidation of glutaminyl and asparaginyl pentapeptides. *J. Pept. Res. 63*, 426−436.
(34) Geiger, T., and Clarke, S. (1986) Deamidation, Isomerization, and Racemization at Asparaginyl and Aspartyl Residues in Peptides. *J. Biol. Chem. 262*, 785−794.
(35) Wakankar, A. A., and Borchardt, R. T. (2006) Formulation considerations for proteins susceptible to asparagine deamidation and aspartate isomerization. *J. Pharm. Sci. 95*, 2321−2336.
(36) Tyler-Cross, R., and Schirch, V. (1991) Effects of amino acid sequence, buffers, and ionic strength on the rate and mechanism of deamidation of asparagine residues in small peptides. *J. Biol. Chem. 266*, 22549−22556.
(37) Runge, S., Thogersen, H., Madsen, K., Lau, J., and Rudolph, R. (2008) Crystal structure of the ligand-bound glucagon-like peptide-1 receptor extracellular domain. *J. Biol. Chem. 283*, 11340−11347.
(38) Fineman, M. S., Mace, K. F., Diamant, M., Darsow, T., Cirincione, B. B., Booker Porter, T. K., Kinninger, L. A., and Trautmann, M. E. (2012) Clinical relevance of anti-exenatide antibodies: safety, efficacy and cross-reactivity with long-term treatment. *Diabetes, Obes. Metab. 14*, 546−554.
(39) Overington, J., Donnelly, D., Johnson, M. S., Sali, A., and Blundell, T. L. (1992) Environment-specific amino acid substitution tables: tertiary templates and prediction of protein folds. *Protein Sci. 1*, 216−226.
(40) Maes, K., Smolders, I., Michotte, Y., and Van Eeckhaut, A. (2014) Strategies to reduce aspecific adsorption of peptides and proteins in liquid chromatography-mass spectrometry based bioanalyses: an overview. *J. Chromatogr. 1358*, 1−13.
(41) Parkes, D. G., Pittner, R., Jodka, C., Smith, P., and Young, A. (2001) Insulinotropic actions of exendin-4 and glucagon-like peptide-1 in vivo and in vitro. *Metab., Clin. Exp. 50*, 583−589.
(42) Cao, Y., Gao, W., and Jusko, W. J. (2012) Pharmacokinetic/pharmacodynamic modeling of GLP-1 in healthy rats. *Pharm. Res. 29*, 1078−1086.
(43) Reid, R., Sgobba, M., Raveh, B., Rastelli, G., Sali, A., and Santi, D. (2015) Analytical and Simulation-Based Models for Drug Release and GelDegradation in a Tetra-PEG Hydrogel Drug-Delivery System. *Macromolecules 48*, 7359−7369.
(44) Shiota, M., and Printz, R. L. (2012) Diabetes in Zucker diabetic fatty rat. *Methods Mol. Biol. 933*, 103−123.
(45) Gedulin, B. R., Smith, P., Prickett, K. S., Tryon, M., Barnhill, S., Reynolds, J., Nielsen, L. L., Parkes, D. G., and Young, A. A. (2005) Dose-response for glycaemic and metabolic changes 28 days after single injection of long-acting release exenatide in diabetic fatty Zucker rats. *Diabetologia 48*, 1380−1385.
(46) Vrang, N., Jelsing, J., Simonsen, L., Jensen, A. E., Thorup, I., Soeborg, H., and Knudsen, L. B. (2012) The effects of 13 wk of liraglutide treatment on endocrine and exocrine pancreas in male and female ZDF rats: a quantitative and qualitative analysis revealing no evidence of drug-induced pancreatitis. *Am. J. Physiol. Endocrinol. Metabol 303*, E253−264.
(47) Jelsing, J., Vrang, N., Hansen, G., Raun, K., Tang-Christensen, M., and Bjerre Knudsen, L. (2012) Liraglutide: short-lived effect on gastric emptying – long lasting effects on body weight. *Diabetes, Obes. Metab. 14*, 531−538.
(48) Santi, D. V., Schneider, E. L., and Ashley, G. W. (2014) Macromolecular prodrug that provides the irinotecan (CPT-11) active-metabolite SN-38 with ultralong half-life, low C(max), and low glucuronide formation. *J. Med. Chem. 57*, 2303−2314.
(49) Fehse, F., Trautmann, M., Holst, J. J., Halseth, A. E., Nanayakkara, N., Nielsen, L. L., Fineman, M. S., Kim, D. D., and Nauck, M. A. (2005) Exenatide augments first- and second-phase insulin secretion in response to intravenous glucose in subjects with type 2 diabetes. *J. Clin. Endocrinol. Metab. 90*, 5991−5997.
(50) Drucker, D. J., Buse, J. B., Taylor, K., Kendall, D. M., Trautmann, M., Zhuang, D., and Porter, L. (2008) Exenatide once weekly versus twice daily for the treatment of type 2 diabetes: a randomised, open-label, non-inferiority study. *Lancet 372*, 1240−1250.
(51) Kim, D., MacConell, L., Zhuang, D., Kothare, P. A., Trautmann, M., Fineman, M., and Taylor, K. (2007) Effects of once-weekly dosing of a long-acting release formulation of exenatide on glucose control and body weight in subjects with type 2 diabetes. *Diabetes Care 30*, 1487−1493.
(52) O'Connor-Semmes, R. L., Lin, J., Hodge, R. J., Andrews, S., Chism, J., Choudhury, A., and Nunez, D. J. (2014) GSK2374697, a novel albumin-binding domain antibody (AlbudAb), extends systemic exposure of exendin-4: first study in humans–PK/PD and safety. *Clin. Pharmacol. Ther. 96*, 704−712.

DOI: 10.1021/acschembio.7b00218
ACS Chem. Biol. 2017, 12, 2107−2116

Supplementary Information

A hydrogel-microsphere drug delivery system that supports once-monthly administration of a GLP-1 receptor agonist

Eric L. Schneider[1], Brian R. Hearn[1], Samuel J. Pfaff[1], Ralph Reid[1], David G. Parkes[2], Niels Vrang[3], Gary W. Ashley[1] and Daniel V. Santi[1,4] *

[1] ProLynx, 455 Mission Bay Blvd. South, Suite 145, San Francisco, CA 94158
[2] DGP Scientific Inc, Del Mar, CA
[3] Gubra ApS, Horsholm Kongevej 11B, 2970 Horsholm, Denmark
[4] Department of Pharmaceutical Chemistry, University of California, San Francisco, 600 16th Street, San Francisco, California 94158, United States

* Corresponding author: Daniel V. Santi, ProLynx, 455 Mission Bay Blvd. South, Suite 145, San Francisco, CA 94158; Daniel.V.Santi@prolynxllc.com. Phone 415 552 5306

Materials and Methods

1. General
2. Peptide synthesis and N-terminal linker attachment
3. Microsphere-peptide conjugates
4. Microsphere-peptide release kinetics
5. GLP-1R assays of [Xaa^{28}]exenatide
6. ELISA
7. *In vitro* exenatide degradation
8. Pharmacokinetics of exenatide versus [Gln^{28}]exenatide
9. Pharmacodynamics of exenatide versus [Gln^{28}]exenatide

Figures and Tables

Figure S1. Cell-based hGLP-1R assays of [Xaa^{28}]exenatides.
Figure S2. GLP-1R bioassays of exenatide and its degradation products.
Figure S3. isoAsp determinations of exenatide reaction mixture and isolated components.
Figure S4. C vs t plots of serum peptides after SC injections of exenatide and [Gln^{28}]exenatide.
Figure S5. Serum [Gln^{28}]exenatide after SC injection of mice with microsphere conjugates.
Figure S6. Insulin levels of varying doses of exenatide and [Gln^{28}]exenatide in OGTTs.
Figure S7. Pharmacodynamic results from the three month study of CI-exenatide and two monthly injections of [Gln^{28}]exenatide-microspheres in ZDF rats.
Figure S8. GLP-1RA serum levels over two months in treated ZDF rats

Table S1. EC_{50} values of synthetic [Xaa^{28}]exenatide in GLP-1R assays and ELISA IC_{50} values.
Table S2. EC_{50} values of synthetic [Asp^{28}]exenatide and exenatide deamidation products in Exendin-4 Bioassay and ELISA IC_{50} values.
Table S3. Pharmacokinetic parameters of exenatide and [Gln^{28}]exenatide in the rat.
Table S4. Pharmacokinetic properties of [Gln^{28}]exenatide-microspheres in the mouse and rat.

1. General.

Samples were analyzed on a Shimadzu LC-20AD HPLC system equipped with an SPD-M20A diode array detector and a Phenomenex Jupiter 5 µm C18 column (300 Å, 150 x 4.6 mm) heated to 40°C. Peaks were eluted with a 15 min linear gradient of 30%-60% MeCN (0.1% TFA) in water (0.1% TFA) at a flow rate of 1 mL/min. Semi-preparative HPLC purifications were performed on the same HPLC system equipped with a Peek Scientific HiQ 5 µm C18 column (50 x 20 mm) heated to 40°C. Products were eluted with a 15 min linear gradient of 30%-60% MeCN (0.1% TFA) in water (0.1% TFA) at a flow rate of 5 mL/min. Preparative HPLC purifications were performed on a Shimadzu Prominence LC-20AP HPLC system equipped with an SPD-M20A UV-VIS detector and a Phenomenex Jupiter 5 µm C18 column (300 Å, 150 x 21.2 mm). Products were eluted with a 15 min linear gradient of 30%-60% MeCN in water (0.1% TFA) at a flow rate of 20 mL/min. UV analyses were performed using a Hewlett-Packard 8453 UV-Vis spectrophotometer or a Thermo Scientific NanoDrop 2000 spectrophotometer. Concentrations of peptide solutions were determined using ε_{280} = 5500 $M^{-1}cm^{-1}$ for the single tryptophan present. ELISA assays were read on a Molecular Devices Spectramax i3 plate reader. *O*-(7-Azido-1-cyano and 1-methylsulfonyl-2-heptyl)-*O*'-succinimidyl carbonates were prepared as reported [1]. Amine-free DMF was obtained by treatment of biotech grade DMF (Sigma 494488) with AldraAmine trapping packets.

2. Peptide synthesis and N-terminal linker attachment.

A. Ambient temperature synthesis of [Xaa^{28}]exenatides. Syntheses were performed on Chemmatrix Rink amide resin (0.5 meq/g) using a Symphony peptide synthesizer. Fmoc-amino acids (5 eq per coupling) were double-coupled to the *N*-terminus of the peptide chain using HCTU (4.9 eq per coupling) and DIPEA (10 eq per coupling) in DMF at ambient temperature. Fmoc groups were removed using 20% 4-methylpiperidine in DMF. [Xaa^{28}]Exenatide was deprotected and cleaved from the resin using 95:2.5:2.5 TFA:TIPS:DTT. HPLC of the crude products indicated a purity of ~15- to 20% of the desired peptides, which were purified to ≥95% purity by preparative HPLC.

[Ala^{28}]exenatide M_{av}: 4143.6 calc; 4143 obsd
[Asp^{28}]exenatide M_{av}: 4187.6 calc; 4187 obsd
[Gln^{28}]exenatide, M_{av}: 4200.6 calc; 4200 obsd
[Lys^{28}]exenatide M_{av}: 4200.6 calc; 4200 obsd

B. Microwave assisted synthesis of NH_2[Gln^{28}]exenatide resin. Synthesis was performed on polystyrene Rink amide AM resin (1.1 meq/g) using a Biotage Initiator + Alstra microwave peptide synthesizer. Fmoc-amino acids (5 eq per coupling) were coupled to the *N*-terminus of the peptide chain using DIC (5 eq per coupling) and oxyma (4.95 eq per coupling) in DMF/NMP at 75°C for 5 min, except for the *N*-terminal histidine, which was reacted at ambient temperature for 30 min. Fmoc groups were removed using 20% 4-methylpiperidine in DMF. After removal of the N-terminal Fmoc, a small amount of [Gln^{28}]exenatide was deprotected and cleaved from the resin using 90:5:5 TFA:TIPS:H_2O. HPLC of the crude products indicated a purity of ~45% of [Gln^{28}]exenatide. M_{av}: 4200.6 calc; 4200 obsd

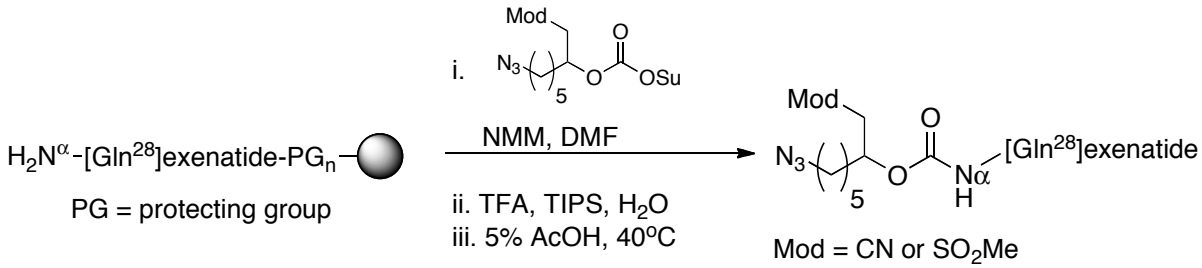

C. Synthesis N^{α}-carbamoyl-[Gln^{28}]exenatide (Mod = -CN and $MeSO_2$-). On-resin *N*-terminal carbamoylation of peptides was performed by a modification of a previously described method [2], and is exemplified by the following.

N^{α}-(7-Azido-1-cyano-2-heptyloxycarbonyl)-[Gln^{28}]exenatide (Mod=-CN).
In a 50 mL SPPS vessel, protected NH_2[Gln^{28}]exenatide (free α-amine) on Rink amide AM resin (1.1 meq/g substitution, 0.14 mmol peptide/g peptide-resin, 2.33 g peptide-resin, 0.33 mmol peptide) was treated with 25 mL of amine-free DMF for 30 min at ambient temperature. The suspension of swollen resin was then treated with 8.0 mL of 0.123 M of *O*-(7-azido-1-cyano-2-heptyl)-*O*'-succinimidyl carbonate (0.32 g, 0.98 mmol, 30 mM final) in amine-free DMF and 4-methylmorpholine (108 µL, 0.98 mmol). The reaction mixture was gently agitated with N_2 bubbling for 2 h. The supernatant was removed by vacuum filtration, and the resin was washed with successively DMF (3 x 15 mL) and CH_2Cl_2 (5 x 15 mL). Kaiser test was negative for free amines in the intermediate linker-modified resin. The resin was then treated with 25 mL of precooled (4°C) 90:5:5 TFA:TIPS:H_2O while gently agitating on an orbital shaker. After 2 h, the resin was vacuum filtered and washed with TFA (2 x 2.5 mL). The filtrate was concentrated by rotary evaporation to ~10 mL. The crude linker-peptide was precipitated by dropwise addition of the TFA concentrate to 100 mL of -20°C MTBE in 4 tared 50 mL Falcon tubes. After keeping at -20°C for 10 min, the crude linker-peptide suspensions were pelleted by centrifugation (4000 x g, 2 min, 4°C), and the supernatants were decanted. The resulting pellets were suspended in 25 mL each (100 mL total) of -20°C MTBE, vortexed to mix, centrifuged, and decanted as above. After drying under high vacuum, the pellets were isolated as off-white solids that were combined (1.6 g) and dissolved in 20 mL of 5% AcOH (80 mg/mL). After heating in a 40°C water bath for 1 h to cleave tryptophan carbamic acid, the crude material was lyophilized then purified by Preparative C18 HPLC to provide 110 mL of an aqueous solution the title compound (0.56 mM, 63 µmol by A_{280}). Lyophilization provided 330 mg of the purified peptide a white solid.

C18 HPLC (A_{280} nm) showed ≥94% purity, RV = 11.7 mL.
M_{av}: 4408.8 calc; 4408 obsd

N^{α}-(7-Azido-1-methylsulfonyl-2-heptyloxycarbonyl)-[Gln^{28}]exenatide (Mod=$MeSO_2$-).
Prepared as above, C18 HPLC determined at 280 nm showed ≥94% purity, RV = 11.5 mL.
M_{av}: 4461.9 calc; 4461 obsd

3. Microsphere-peptide conjugates.

The 40 µm amino and MFCO-derivatized microspheres were prepared and handled aseptically as described [2]. Cleavable polymer crosslinks contained the following modulators [1, 3]: $(CH_3OCH_2CH_2)_2NSO_2$- when drug release was controlled by the $MeSO_2$-modulator, $(CH_3CH_2)_2NSO_2$- for rat PK studies or $(CH_3OCH_2CH_2)_2NSO_2$- for rat PD

studies when drug release used the –CN modulator. The SPAAC coupling, washing and aseptic transfers of reagents were performed in the syringe-to-syringe transfer reaction vessel described [2] by the following exemplary procedure.

To a suspension of 2.4 g of a slurry of MFCO-derivatized microsphere (11.2 μmol MFCO) in H_2O 0.05% Tween 20 in a 10 mL syringe was added a solution of 46 mg (10.4 μmol) of N^{α}-[1-(methylsulfonyl)-7-azido-2-heptyloxycarbonyl]-exenatide in 2 mL H_2O 0.05% Tween 20. The mixture was slowly rotated until the OD_{280} of an aliquot was constant at ~24 hr. About 50% of the slurry was syringe-to-syringe transferred to a second syringe, and both samples were washed with 5 x 6 mL of H_2O 0.05% Tween 20 and then 5 x 6 mL of isotonic acetate (10 mM Na Acetate, 143 mM NaCl) pH 5.0 0.05% Tween 20. The total loading of the microsphere was 2.2 μmol exenatide gm^{-1} of slurry as determined by the total peptide released at pH 8.4 (below).

4. Microsphere-peptide release kinetics.

Kinetics of β-elimination were determined in duplicate under accelerated release conditions using 50 mg of the microsphere-peptide slurry in 500 μL of 100 mM Bicine, pH 8.4 or CHES at pH 9.4 at 37 °C. At time intervals, samples were centrifuged at 20,000 x g in a microfuge tube and A_{280} of the supernatant was measured on a NanoDrop 2000 spectrophotometer (ThermoScientific) at intervals. The release rate was calculated by fitting the released A_{280} vs time to the first-order rate equation. Knowing that the β-elimination is first-order in hydroxide ion [1] rates were calculated at pH 7.4 as $k_{pH\ 7.4} = k_{pH} \times 10^{(pH-7.4)}$.

5. GLP-1R assays of [Xaa^{28}]exenatide. GLP-1R assays were performed using the frog melanophore assay [4] and cAMP Hunter assay (DiscoverX, Freemont, CA).

A. Melanophore bioassay. For melanophore bioassays, human GLP-1R was transiently expressed in *X. laevis* cells, then aliquots of a 12-point 3-fold dilution series of peptide were added to wells of a 96-well plate containing cells and assayed for GLP-1R activation; complete details of the assay have been reported [5]. **Fig. S1A** shows the results of GLP-1R cell-based melanophore assays of [Xaa^{28}]exenatides and **Table S1** summarizes EC_{50} values.

B. cAMP Hunter eXpress assay of hGLP-1R. The cAMP Hunter eXpress GLP-1R CHO-K1 assays (DiscoveRx) were performed using kits and instructions provided by the manufacturer. The results are given in **Fig. S1B** and EC_{50} values summarized in **Table S1**.

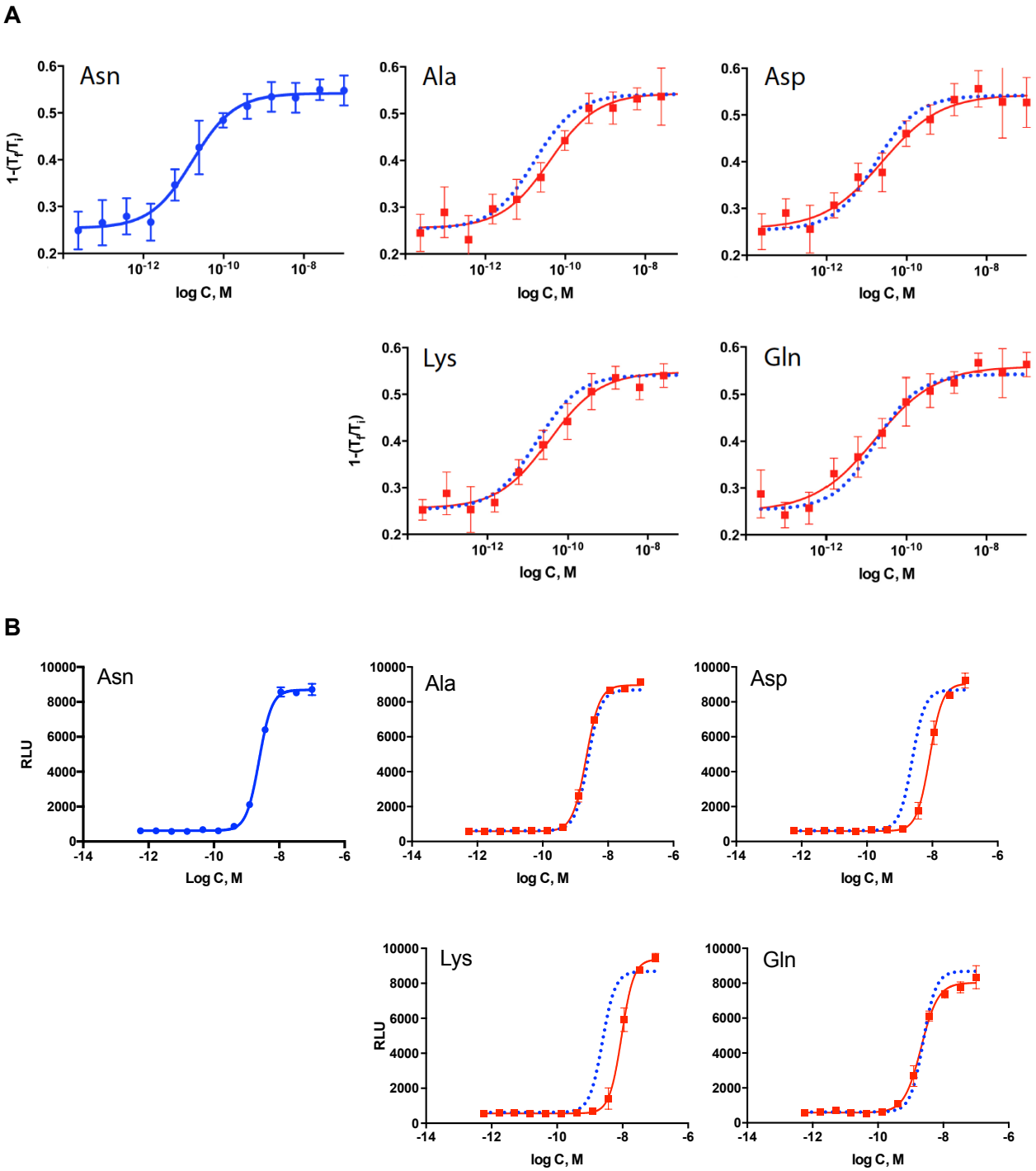

Figure S1. Cell-based hGLP-1R assays of [Xaa^{28}]exenatides. A) Dose-response curves using the melanophore bioassay using *S. Laevis* cells; T_i is the initial baseline read and T_f is the response read. B) Dose-response curves using the cAMP Hunter bioassay with hGLP-1R expressed in CHO-K1 cells (DiscoverX kit 95-0062Y2BG2E); RLU, relative luminescent units. The exenatide control curve in the first panel of each assay is reproduced in each curve as a blue dotted line (---). Data were fit to a four-parameter logistic model (solid lines); points are averages ± SD.

Table S1. EC_{50} values of synthetic [Xaa^{28}]exenatide in GLP-1R assays and IC_{50} values from ELISAs.

Xaa^{28}	**GLP-1R agonist assay** [A]		**ELISA** [A]
	Melanophore bioassay EC_{50}, pM	**cAMP Hunter bioassay EC_{50}, nM**	**IC_{50}, nM**
Asn (exenatide)	17 ±3.4	2.4 ±0.12	0.21 ±0.04
Ala	41 ±10	2.1 ±0.11	6.0 ±0.09
Asp	25 ±8.4	8.3 ±0.74	>100
Lys	35 ±7.6	9.3 ±0.70	>100
Gln	16 ±5.0	2.1 ±0.28	11 ±3.7

[A] Data were fit to a four-parameter logistic model using Graphpad Prism. Values are best fits ± SE of the fits.

6. ELISA

The competitive ELISA (Peninsula Lab S1310) was performed as recommended by the supplier. **Table S1** provides IC_{50} values of various [Xaa^{28}]exenatides.

7. *In vitro* exenatide degradation

A solution of 2.4 mM exenatide (1 mL; 13.2 A_{280}), 0.1% NaN_3 and 200 M Lys(DNP)OH in 200 mM NaP_i, pH 7.4, 37 °C, was incubated for 56 days. At intervals, 50 µL aliquots were removed and frozen at -20 °C. Various samples were thawed and analyzed a) by HPLC, b) by competitive ELISA, c) for GLP-1R agonist activity, and d) for protein isoaspartate methyl transferase (PIMT) activity. The sample incubated for t= 56 days was subjected to HPLC and samples at RV 9.9, 10.4 and 10.8 were collected and individually analyzed for purity by analytical RP-HPLC, and for GLP-1R agonist and PIMT activity.

A) Exenatide degradation. HPLC profiles of the deamidation of exenatide vs time are shown in Fig. 1 of text. Each peak at t=56 day was purified by RP-HPLC. Analytical HPLC showed that the isolated L-Asp and D-isoAsp peaks still contained ~7 and 12% contaminating IsoAsp, respectively, and ELISA indicated ~14% exenatide remained in the co-eluting [Asp^{28}]exenatide (see below); the isolated [L-$isoAsp^{28}$]exenatide showed a single peak on analytical HPLC.

B) ELISA of degradation products. Competitive ELISA IC_{50} values of synthetic [Asp^{28}]exenatide and isolated HPLC peaks of [Asp^{28}]- and [$isoAsp^{28}$]exenatide are given in **Table S2**. Although synthetic [Asp^{28}]exenatide bound poorly to the antibody used, the Asp^{28} peptide isolated from the reaction mixture showed an IC_{50} 6.7-fold higher than exenatide, which was accounted for by ~14% exenatide contamination.

C) GLP-1R assays of degradation products. GLP-1R cAMP Hunter bioassays (DiscoverX) of exenatide, its degradation products and synthetic [Asp^{28}]exenatide are provided in **Fig. S2**. Shown are dose response curves for the complete reaction solutions at t= 0 and 56 days, and from isolated fractions corrected for A_{280}. The EC_{50} values are summarized in **Table S2**. As above, the L-Asp peptide isolated from the

deamidation mixture contained low levels of exenatide and the L-isoAsp peptide. The amount of D-isoAsp formed in the deamidation at t=56 days was so small (~12%) it would not contribute significantly to agonist activity of the crude mixture.

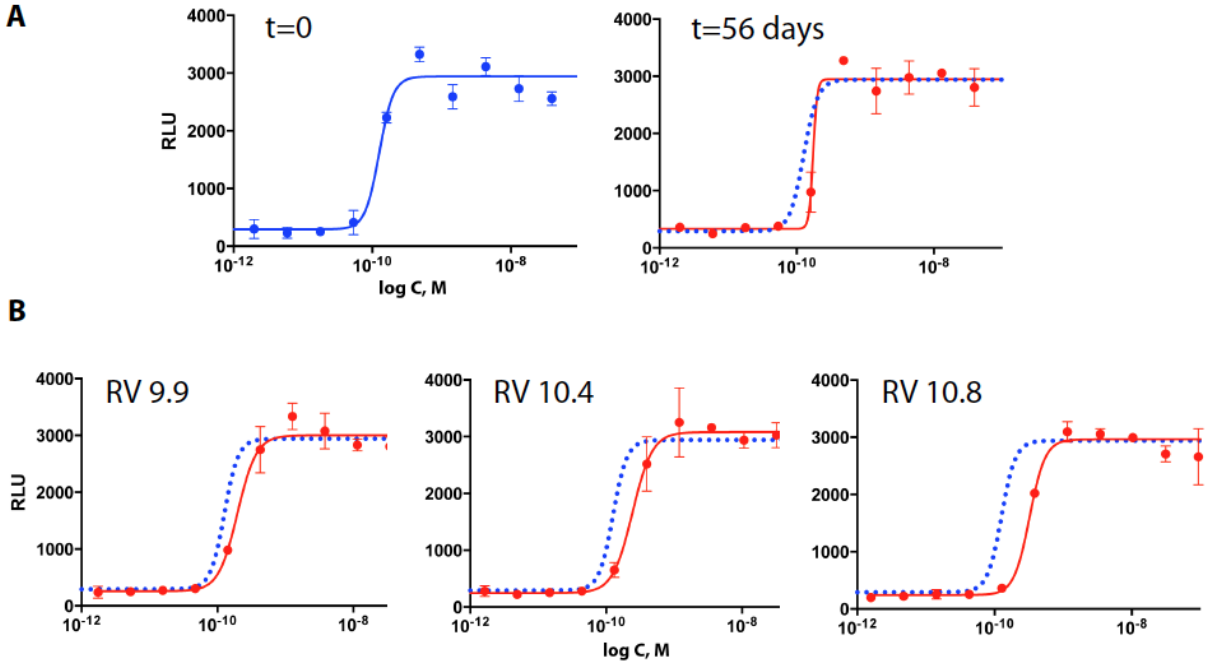

Figure S2. GLP-1R cAMP Hunter bioassay of exenatide and its crude and purified degradation products. A) Starting (t=0) and final (t=56) reaction mixes. B) Isolated components of mixture. RLU, relative luminescent units. The exenatide control curve is reproduced in each curve as a blue dotted line (---). Data were fit to a four-parameter logistic model (solid lines); points are averages ± SD.

Table S2. EC_{50} values of synthetic [Asp^{28}]exenatide and exenatide deamidation products in cAMP Hunter Exendin-4 Bioassay and ELISA IC_{50} values (Peninsula Lab. S1310).

Xaa^{28}	**GLP-1R**		**ELISA**
	EC_{50}, pM [A]	**Relative EC_{50}**	**IC_{50}, nM**
Asn, Exenatide (t=0)	130 ±26	1	0.21 ±0.04
Product mixture (t= 56 days)	173 ±31	1.3	ND
L-Asp (RV 9.8)	[B] 197 ±22	1.5	[B] 1.4 ±0.09
L-Asp (synthetic)	–	[C] 1.5-3.5	>100
D-isoAsp (RV 10.4)	[B] 244 ±25	1.9	ND
L-isoAsp (RV 10.8)	324 ±35	2.5	40 ±7

[A] Differences from EC_{50} values shown in Table S1 are attributed to different cell batches used. [B] isolated L-Asp and D-isoAsp values are uncorrected for isoAsp and/or exenatide impurities. [C] Estimated using data from **Table S1**. Data were fit to a four-parameter logistic model using Graphpad Prism; values are best fits ± SE of the fits.

D) Isoaspartate analysis of degradation products. Protein isoaspartate methyl transferase (PIMT) assays were performed using the ISOQUANT isoaspartate detection kit as recommended by the supplier (Promega). Sample mixtures at t=0 and t = 56 days, as well as individual samples purified by HPLC from the t= 56 day mixture were assayed for IsoAsp peptides. **Fig. S3** shows the AdoHCys/peptide specific activity formed in a)

the total mixture and in b) isolated peaks at t= 56 days after adjustment for small amounts of contaminating [isoAsp^{28}]exenatide contaminant (see HPLC, **Fig. 2** of text)).

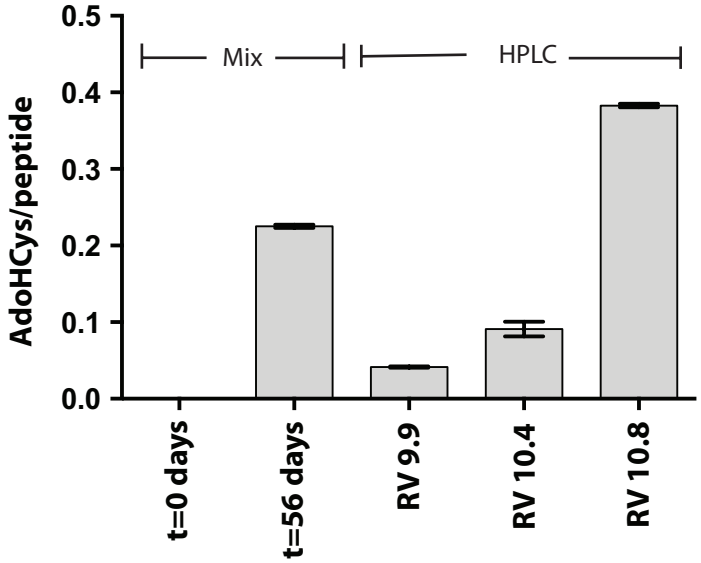

Figure S3. IsoAsp determinations of exenatide reaction mixture at t= 0 and 56 days, and isolated components of the degradation mix at 56 days. Values for L-Asp- and D-isoAsp-containing peptides were adjusted for the small amounts of L-isoAsp-peptide detected by HPLC in the samples. The residual PIMT-positive peaks at RV 9.9 and 10.4 are attributed to low-level [L-isoAsp^{28}]exenatide impurities in the isolated HPLC fractions. Error bars are ±SD.

8. Pharmacokinetics of exenatide versus [Gln^{28}]exenatide.

Animal pharmacokinetic experiments were performed at MuriGenics and conformed to IACUC recommendations.

A. Pharmacokinetics of exenatide and [Gln^{28}]exenatide in the rat. Solutions of exenatide (80 µg/mL) and [Gln^{28}]exenatide (49 µg/mL), determined by A_{280} (ε_{280} = 5,500 $M^{-1}cm^{-1}$), were prepared in sterile 10 mM NaOAc, pH 4.5, and filtered through a sterile, centrifugal spin filter (0.2 µm). Normal, male Sprague Dawley rats with jugular cannulas (average weight 254 g) were dosed with either 80 µg/kg exenatide or 49 µg/kg [Gln^{28}]exenatide SC in the flank (n = 3 rats for each peptide) or IV through the cannula (n = 3 rats for each peptide). Blood samples were drawn pre-dose and at 10 min, 30 min, 1 h, 2 h, 3 h, 4 h, 6 h, 8 h and 24 h after dosing. Serum was prepared and frozen at -80 ^{o}C until analysis. Serum exenatide and [Gln^{28}]exenatide was analyzed by LC/MS/MS. In the C vs t plots presented in the text (**Fig. 3**) k values were obtained using Graphpad Prism by non-linear regression using a single-phase decay model with weighting by $1/SD^2$; all other values were determined in Winnonlin using non-compartmental analysis with weighting by $1/Y^2$. The derived pharmacokinetic parameters are summarized in **Table S3**.

Table S3. Pharmacokinetic parameters of exenatide and [Gln^{28}]exenatide in the rat

	exenatide [A]		**[Gln^{28}]exenatide** [B]	
	IV	SC	IV	SC
C_{max}, nM	45 ± 11	20 ± 3	29 ± 4	10 ± 2

k, hr^{-1}	2.4 ±0.04	0.7 ±0.1	2.5 ±0.2	0.6 ±0.1
$t_{1/2,}$ min	18	50	17	48
V_{inf}, L/kg	0.27 ± 0.05		0.27 ± 0.02	
AUC, nM-hr/dose	30 ± 4	21 ± 3	19 ± 2	12± 2
Clearance, L/hr/kg	0.64 ± 0.09		0.63 ± 0.06	
Clearance/F, L/hr/kg		0.9 ± 0.1		1.0 ± 0.2
Dose-adjusted				
$C_{max,DA}$, nM-kg/nmol	2.4 ± 0.6	1.1 ± 0.2	2.5 ± 0.3	0.9 ± 0.2
AUC_{DA}, nM-hr*kg/nmol	1.6 ± 0.2	1.1 ± 0.2	1.6 ± 0.2	1.0 ± 0.2
Bioavailability (F)		0.69		0.62

[A] 19.1 nmol/kg exenatide (80 µg/kg) was injected either IV or SC and measured by LC/MS/MS. [B] 11.7 nmol/kg [Gln^{28}]exenatide (49 µg/kg, ~12 µg/rat) was injected either IV or SC and measured by LC/MS/MS. The $t_{1/2}$ values are derived from best-fit rates ±SE; other values are mean ±SD.

B. Pharmacokinetics of exenatide and [Gln^{28}]exenatide in the mouse. A solution of [Gln^{28}]exenatide (90 µg/mL) was prepared in sterile PBS with 1 mg/mL BSA, pH 7.4, and filtered through a sterile, centrifugal spin filter (0.2 µm). Normal CD-1 mice (average weight 39 g) were dosed with 90 µg/kg (21.4 nmol/kg, ~3.5 µg/mouse) [Gln^{28}]exenatide SC in the flank. Serum samples used for analysis were obtained pre-dose and at 10 min, 30 min, 1 h and 2 h after dosing; samples were collected from 12 animals using 3 mice per time point and frozen at -80 °C until analysis by LC/MS/MS. C vs t plots of the data are shown in **Fig. S4**.

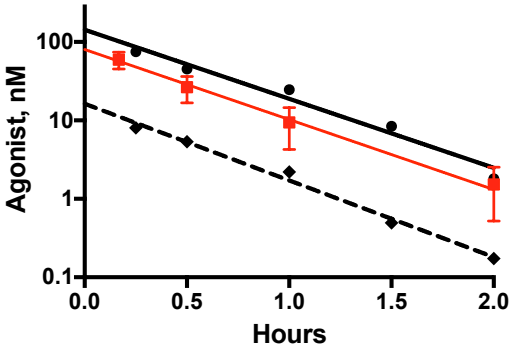

Figure S4. C vs t plots of serum peptides after SC injections of 200 µg/kg (-●-) and 20 (--◆--) µg/kg of exenatide, and 90 µg/kg of [Gln^{28}]exenatide (-■-) in the mouse. From top to bottom, $t_{1/2,\beta}$ values are 20.5-, 20.2- and 18.5 min. For [Gln^{28}]exenatide, the C vs t curve was analyzed using Graphpad Prism by non-linear regression using a single-phase decay model with weighting by $1/SD^2$. Points are the average values from 3 mice per time point and error bars show ±SD. The calculated elimination k_β = 2.06 hr^{-1} ±0.11 (SE), V_z/F = 0.36 ± 0.09 (SD) L/kg and $AUC_{0\text{-}2hr}$ = 34 ±4 (SD) nM*hr. Data for exenatide are from U.S. FDA. Center for Drug Evaluation and Research. Application number 21-773 Pharmacology review.

C. Pharmacokinetics of hydrogel-microsphere [Gln^{28}]exenatide conjugates in the rat. Syringes (0.5 mL U-100 insulin syringe with fixed 29g x ½" needle, BD) were filled under sterile conditions with the [Gln^{28}]exenatide-microsphere slurry in isotonic acetate (10 mM

Na Acetate, 143 mM NaCl) pH 5.0 0.05% Tween 20. Microspheres using Mod=$MeSO_2$- contained 1.3 μmol [Gln^{28}]exenatide/g slurry, and microspheres using Mod=CN contained 1.4 μmol [Gln^{28}]exenatide/g slurry. The content of each syringe was administered SC in the flank of six cannulated male Sprague Dawley rats (average weight 270 g). The needle assembly was purged of air and weighed prior to and following dosing to determine the mass of the slurry delivered to each rat; with the $MeSO_2$ modulator 130 mg slurry containing 0.7 mg [Gln^{28}]exenatide (170 nmol) was administered to each rat, and with the CN modulator 400 mg slurry containing 2.5 mg [Gln^{28}]exenatide (580 nmol) was administered. Blood samples (300 μL) were drawn at 0, 1, 2, 4, 8, 24, 48, 72, 120, 168, 240, 336, 432, 504, 600, 672 h for both linkers and additional samples were obtained at 840, 1008, 1176, 1344, 1512, 1680, 1848, and 2016 h for the linker with Mod = CN. Serum was prepared and frozen at -80 °C until analysis. Serum [Gln^{28}]exenatide was analyzed by LC/MS/MS.

The C vs t curves (text) were analyzed using Graphpad Prism by non-linear regression of eq 1 (text) with weighting by $1/SD^2$; here, since $k_a >> k_1$ we modeled the single exponential phase of the terminal half-life using data points after ~two days. Pharmacokinetic parameters are summarized in **Table S4**.

Table S4. Pharmacokinetic properties of hydrogel-[Gln^{28}]exenatide microspheres in the mouse and rat.

	Mouse		**Rat**	
Modulator	**$MeSO_2$-**	**-CN**	**$MeSO_2$-**	**-CN**
Dose, umol/kg	0.94	4.5	0.68	2.2
C_{max} ± SE, nM	2.7 ± 0.5	0.85 ± 0.08	3.3 ± 0.4	0.51 ± 0.04
k ± SE, hr^{-1} [A]	28 ± 3.9	9.5 ± 1.0	22 ±1.6	7.8 ± 1.3
$t_{1/2,}$ hr	244	730	310	880
AUC_{inf}, nM-hr	852	1010	783	480
AUC_{last} ± SE, nM-hr [B]	730 ± 55	820 ± 72	720 ± 19	340 ± 18
Dose-adjusted				
$C_{max,DA}$, nM*kg/umol	2.9	0.18	4.7	0.24
$AUC_{inf, DA}$, nM-hr*kg/umol	900	230	1120	230

[A] The k and $t_{1/2}$ values are derived from best-fit rates ±SE. All other values were determined in Winnonlin using sparse-sampling non-compartmental analysis with weighting by $1/Y^2$. [B] In the mouse, AUC_{last} is AUC_{0-28} days for $MeSO_2$- and AUC_{0-77} days for –CN; in the rat, AUC_{last} is AUC_{0-42} days for $MeSO_2$- and AUC_{0-84} days for –CN.

D. Pharmacokinetics of hydrogel-microsphere [Gln^{28}]exenatide conjugates in the mouse.
The small amounts of microspheres needed in the mouse required a diluent to allow accurate dosing. Using a dual syringe-based reaction vessel [2] the buffer of a [Gln^{28}]exenatide-microsphere slurry (~1 mL for Mod = $MeSO_2$-, 4 mL for –CN) was aseptically exchanged for a solution of isotonic acetate pH 5.0 (10 mM NaOAc, 143 mM NaCl), 25% glycerol and 0.05% Tween 20. This diluent served to keep the microspheres in a homogeneous suspension prior to and during administration and allowed dosing of convenient volumes. The slurry was then diluted with the same mixture to give 264 nmol [Gln^{28}]exenatide/mg slurry (Mod=$MeSO_2$-) or 720 nmol [Gln^{28}]exenatide/mg slurry

(Mod=CN). Syringes (0.5 mL U-100 insulin syringe with fixed 29 g x ½" needle, BD) were filled with the suspended microspheres under aseptic conditions. The needle assembly of each syringe was purged of air and weighed prior to and following dosing to determine the average mass of slurry delivered to each mouse.

For Mod=$MeSO_2$-, 120 mg of slurry containing 130 µg [Gln^{28}]exenatide (30 nmol) was administered SC in the flank of each of 18 CD-1 mice (average weight 30 g). Blood samples (100 µL) were drawn from the orbital sinus at 8, 24, 48, 72, 96, 120, 168, 240, 336, 408, 504, 576 and 672 h on a staggered schedule to give 6 replicates at each time-point, and sera of each were prepared. For Mod=CN, 200 mg slurry containing 605 µg [Gln^{28}]exenatide (144 nmol) was likewise administered SC to 24 CD-1 mice. Blood samples (100 µL) were drawn from the orbital sinus at the same times as above, and also at 840, 1008, 1176, 1344, 1512, 1680, 1848, and 2016 h on a staggered schedule to give 6 replicates at each time-point. Serum was prepared and frozen at -80 °C until analysis. Serum [Gln^{28}]exenatide was analyzed by LC/MS/MS.

The C vs t plots for the mouse are presented in **Fig. S5**. Values for k were obtained using Graphpad Prism by non-linear regression using a single-phase decay model with weighting by $1/SD^2$; since $k_a >> k_1$ we modeled the single exponential phase of the terminal half-life using data points later than the first few days. Pharmacokinetic parameters are summarized in **Table S4**.

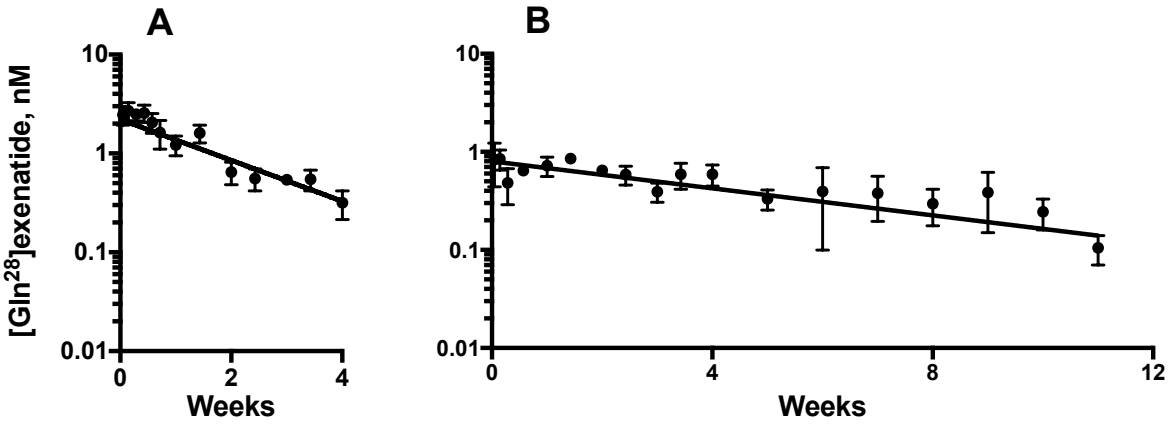

Figure S5. Serum [Gln^{28}]exenatide levels after SC injection of mice with microsphere conjugates. A) After injection with hydrogel-[Gln^{28}]exenatide microspheres with a $MeSO_2$- modulator (30 nmol [Gln^{28}]exenatide/mouse or 4.2 mg /kg); $t_{1/2,\beta}$ was 244 hr. B) After injection with hydrogel-[Gln^{28}]exenatide microspheres with a -CN modulator (144 nmol [Gln^{28}]exenatide/mouse or 20 mg/kg); $t_{1/2,\beta}$ was 730 hr. Error bars are ±SEM.

E. LC-MS/MS analysis of [Gln^{28}]exenatide. [Gln^{28}]exenatide concentrations were measured by LC/MS-MS at Medpace analytical. 50 µL rat serum samples were treated with 3 vol of ACN and centrifuged. The supernatant was dried, reconstituted and applied to a HPLC MS/MS system. The sample was eluted by a water/ACN gradient containing 0.1% formic acid. The calibration curve for exenatide N28Q was linear over the range of 0.25 - 100 ng/mL. HPLC-MS/MS analyses were carried out on a Sciex 5500 Q Trap mass spectrometer coupled with a Shimadzu HPLC system. The Shimadzu HPLC system consisted of two LC-30AD HPLC pumps and a SIL-30AC autosampler with a 100-µL loop installed. The chromatographic separations were achieved on a 3-µm C18,

2.1×50 mm HPLC column, with mobile phase gradients. The mass spectrometer was operated in positive electrospray ionization mode and the resolution setting used was the unit for both Q1 and Q3. The multiple-reactions monitoring (MRM) transition was m/z = 841.1 ->396.3 for exenatide N28Q. Peak-area integrations were performed using Analyst software v1.5.2 from Sciex. The LOQ for [Gln^{28}]exenatide was 0.25 ng/mL.

9. Pharmacodynamics of exenatide versus [Gln^{28}]exenatide.

Animal experiments were performed at Gubra ApS and conformed to international accepted principles for the care and use of laboratory animals. All experiments were covered by a personal license for Jacob Jelsing (2013-15-2934-00784) issued by the Danish Committee for animal research.

A. Acute oral glucose tolerance test (OGTT) after exenatide and [Gln^{28}]exenatide administration. A total of 96 male C57BL/6J mice were obtained at the age of 7 wks from Janvier (JanVier Labs, France) Mice were single housed upon arrival at the Gubra animal facilities and acclimatized for one wk under a 12:12-hr light-dark cycle with free access to food (standard rodent chow, Altromin 1234) and water. Mice were stratified according to body weight at day -1 into 16 groups of n=6. On the day of experimentation (day 0) mice were first semi-fasted 4 hours before glucose bolus (t=-240 min) in clean cages then injected SC at t -30 min with either vehicle (PBS+0.1%BSA) or 0.03, 0.1, 0.3, 1, 3, 10 and 20 µg/kg of each exenatide or [Gln^{28}]exenatide peptide before 2g/kg (at 5 ml/kg) glucose was administered PO at t=0. Blood glucose was measured at t= -60, -30, 0, 15, 30, 60 and 240 min, and insulin measured at t= 15 min.

Blood samples for blood glucose measurements were collected into heparinized glass capillary tubes and immediately suspended in glucose/lactate system solution buffer (EKF-diagnostics, Germany). BG was measured using a BIOSEN c-Line glucose meter (EKF diagnostics, Germany) according to the manufacturer's instructions. Blood samples for insulin measurements were collected in heparinized tubes and plasma separated and stored at -80˚C until analysis. Insulin was measured in duplicates using the MSD platform (Meso Scale Diagnostics) according to the manufacturer's instructions.

The OGTT blood glucose results are presented in the text, and insulin AUC levels at t= 15 min are shown in **Fig. S6**.

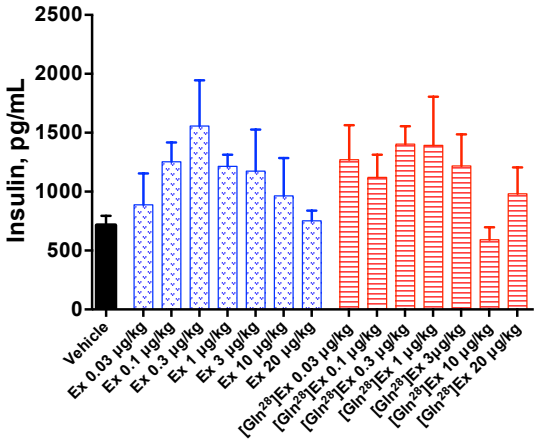

Figure S6. Insulin levels of varying doses of exenatide (Ex) and [Gln^{28}]exenatide 15 min after administering glucose in the OGTT. Data shown as mean +SEM (n=5-6/group). One-way ANOVA followed by Fisher´s post hoc test (NS).

B. Chronic glucoregulatory effects of [Gln^{28}]exenatide-microspheres injected Q4Wk vs exenatide continuous infusion. Fifty-five male Zucker diabetic fatty rats (ZDF-Lepr^{fa}/Crl; Charles River, USA) were obtained at the age of 6 wks. Upon arrival animals were single housed at a target temperature of 22 ±2 °C, relative humidity 50 ±10%, with a 12:12-hr light-dark cycle. Animals were provided with bedding, nesting, and a hide for environmental enrichment. Rats had free access to Purina 5008 chow (Brogaarden) and water during the entire study period unless otherwise stated. For the first 2 wks body-weight and glucose (morning fed) was determined bi-weekly. Following 3.5 wks most animals developed diabetes and out of 55 animals 40 diabetic rats (average weight 340 g, blood glucose 9.7 to 22.5 mM, average 16.2 mM) were stratified into 4 groups of n=10 based on blood glucose and HbA1c levels determined day -1. At day 0 animals were subcutaneously implanted with Alzet minipumps in the neck region under isoflurane anaesthesia. Groups were treated as follows: 1) Alzet pump vehicle control (50mM NaOAc, pH 4.5); 2) Alzet pump with exenatide dissolved in vehicle (30 µg/kg/day); 3) Alzet pumps vehicle + SC microsphere-[Gln^{28}]exenatide at 920 µg/kg (0.22 µmol/kg); and 4) Alzet pump vehicle and SC microsphere-[Gln^{28}]exenatide at 9200 µg/kg (2.2 µmol/kg). Body-weight was recorded daily, food and water intake was recorded daily for the first 2 wks then bi-weekly, and glucose was measured bi-weekly (morning fed glucose). On day 29, pumps were replaced and [Gln^{28}]exenatide was re-dosed SC at the same levels. On day 56, the pumps were removed and animals were allowed to recover for an additional 4 wks before termination.

Blood sampling was performed for pharmacokinetic studies 2 days after the first dose and then once weekly. Glucose samples were collected into 10 ml heparinized glass capillaries and analyzed on the test day using a BIOSEN c-Line glucose analyzer. Insulin samples (75 µl blood) were collected into heparinized tubes, plasma separated and samples subsequently analyzed using an AlphaLisa (PerkinElmer, Skovlunde, Denmark) according to the manufacturer's instructions. HbA1c and acetaminophen were measured using a Cobas c-111autoanalyzer with commercial kits (Roche Diagnostics, Mannheim, Germany) according to instructions. HbA1c was measured day -3, and days 26 and 55 before the gastric emptying test (for further details see Ref. [6]) and OGTT and the gastric emptying test was performed on day 26. On day 55 a terminal OGTT was

performed. In brief, rats were semi-fasted overnight, offered 60% of average 24 hr food intake the night before the OGTT, then PO glucose (2 g/kg) was administered at a volume of 10ml/kg at t=0 min. Blood glucose and insulin were measured at t= -60, 0, 15, 30, 60, 120 and at day 26 and also at -15 and 240 minutes on day 55 after the glucose challenge. Gastric emptying was measured by administration of acetaminophen (100 mg/kg) with the OGTT on day 26, and blood levels were measured at 15, 30, 60 and 120 min.

Complete data from the chronic pharmacodynamic study are shown in **Fig. S7**. OGTT AUC values for day 55 are presented for both 3 and 5 hour time spans (**Fig. S7J,L**). Blood glucose, HbA1c changes and glucose and insulin from the OGTT are presented in the text. C vs t plots of serum peptides at weekly intervals are shown in **Fig. S8.**

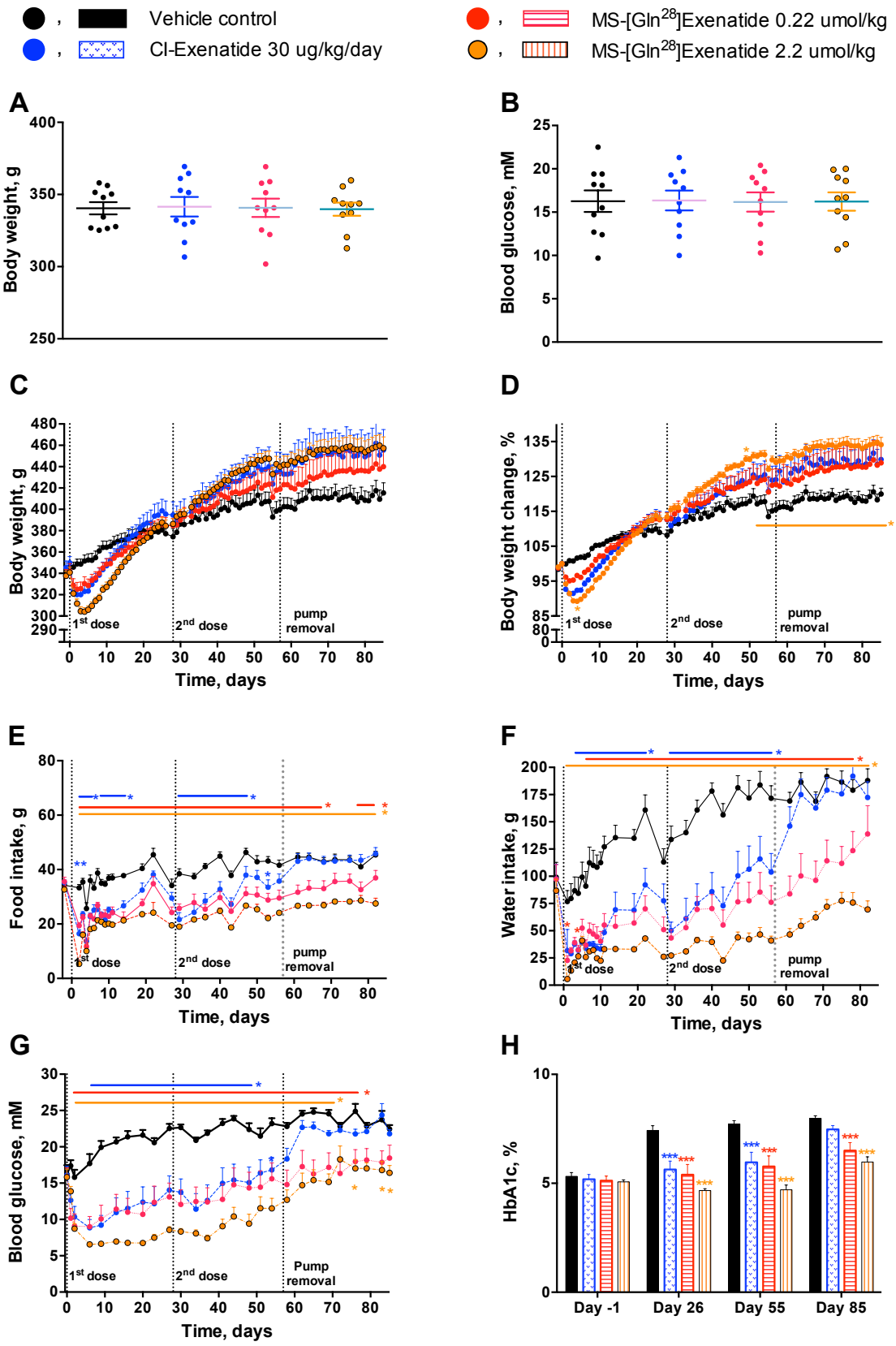
Vehicle control
Cl-Exenatide 30 ug/kg/day
MS-[Gln28]Exenatide 0.22 umol/kg
MS-[Gln28]Exenatide 2.2 umol/kg
A
Body weight, g
B
Blood glucose, mM
C
Body weight, g
1st dose
2nd dose
pump removal
Time, days
D
Body weight change, %
1st dose
2nd dose
pump removal
Time, days
E
Food intake, g
1st dose
2nd dose
pump removal
Time, days
F
Water intake, g
1st dose
2nd dose
pump removal
Time, days
G
Blood glucose, mM
1st dose
2nd dose
Pump removal
Time, days
H
HbA1c, %
Day -1
Day 26
Day 55
Day 85

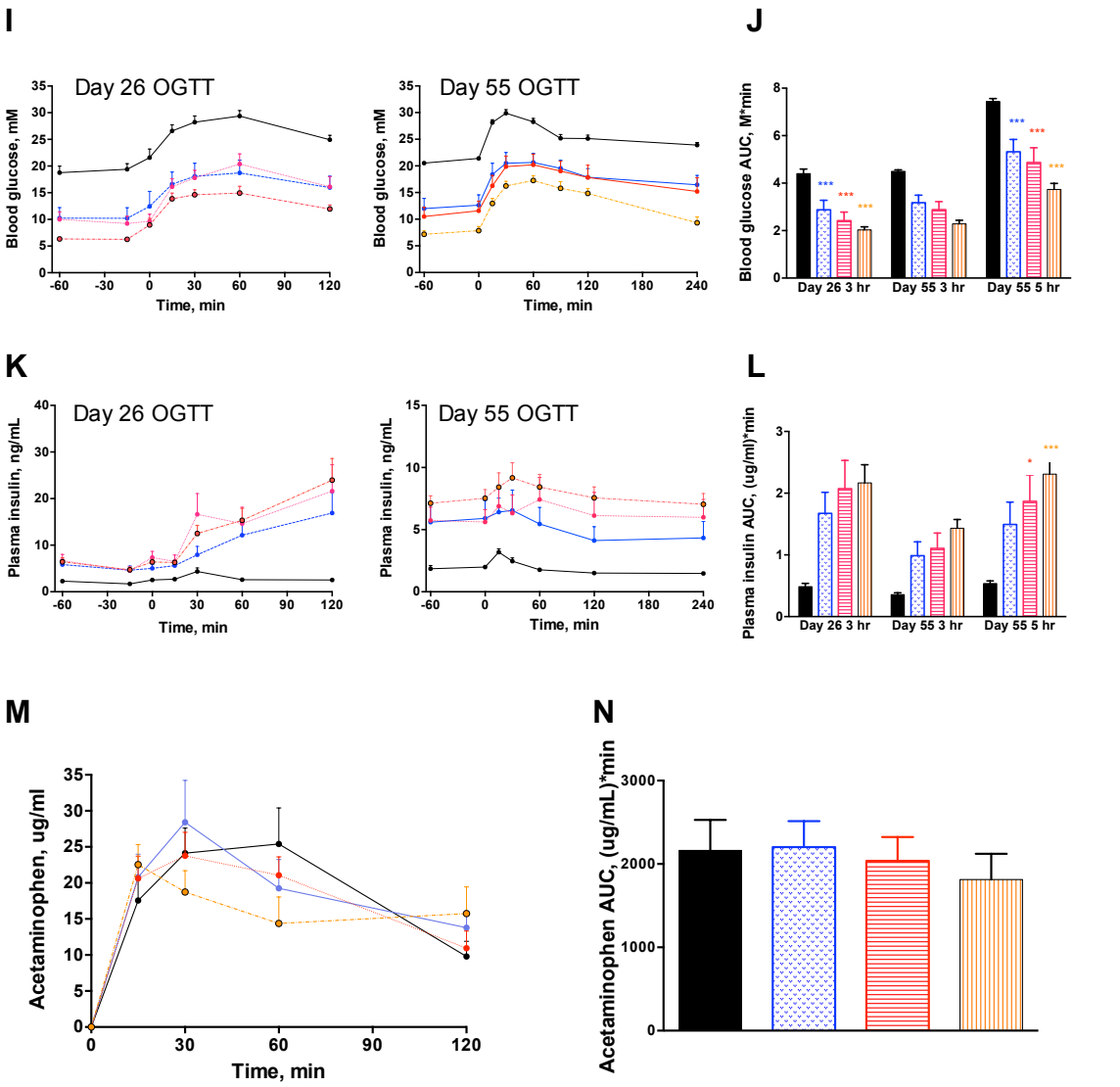

Figure S7. Pharmacodynamic results from the three month study of CI-exenatide and two monthly injections of [Gln^{28}]exenatide-microspheres in male ZDF rats. Key is at top of figure, and vertical dotted lines show dosing at days 0 and 26 and removal of pumps at day 57. (A) Body weight and (B) blood glucose of stratified groups. (C) Body weight and (D) body weight change over the 12 weeks. (E) Food and (F) water intake over the 12 weeks. (G) Blood glucose over 12 weeks and (H) %HbA1c at days -1, 26, 55 and 85. (I) OGTT blood glucose levels and (J) blood glucose AUC values at days 26 and 55 as determined over 3 or 5 hours at day 55. (K) OGTT insulin levels and (L) insulin AUC values at days 26 and 55, as determined over 3 or 5 hours at day 55. (M) Gastric emptying: acetaminophen levels and (N) AUC values at day 26. All data shown as mean +SEM. Data analyzed by one-way ANOVA (bar-graphs) or two-way repeated measures ANOVA (line-graphs) with Bonferroni post-hoc test; * p<0.05, ** p<0.01, *** p<0.001.

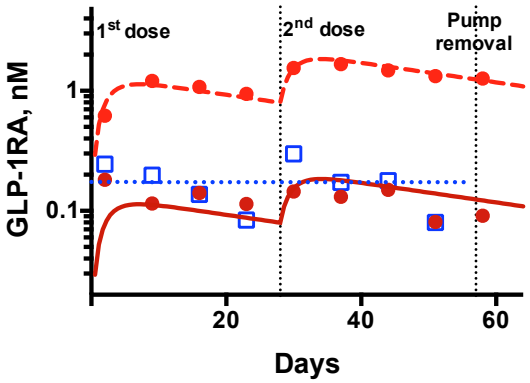

Figure S8. GLP-1RA serum levels over two months in treated ZDF rats. CI-infusion of 30 ug/kg/day exenatide (□), two monthly SC injections of microspheres carrying 9200 µg/kg (- -●- -) and 920 µg/kg (–●–) of microsphere-[Gln^{28}]exenatide. Sera from 5 rats were combined and analyzed by LC-MS/MS. For [Gln^{28}]exenatide, the sparsely sampled C vs t curves were modeled by superposition of curves for single injections, generated from eq. 1 using $t_{1/2,1}$ = 880 h and optimizing CL/F to 1.33 L/h/kg. For CI-exenatide, the average concentration (170 pM) for days 0-56 is shown by a dotted line; after removal of the pump at 57 days exenatide levels rapidly dropped below the LLOQ.

References

1. Santi, D. V., Schneider, E. L., Reid, R., Robinson, L., and Ashley, G. W. (2012) Predictable and tunable half-life extension of therapeutic agents by controlled chemical release from macromolecular conjugates, *Proc. Natl. Acad. Sci. USA 109*, 6211-6216.

2. Schneider, E. L., Henise, J., Reid, R., Ashley, G. W., and Santi, D. V. (2016) Hydrogel Drug Delivery System Using Self-Cleaving Covalent Linkers for Once-a-Week Administration of Exenatide, *Bioconj. Chem. 27*, 1210-1215.

3. Ashley, G. W., Henise, J., Reid, R., and Santi, D. V. (2013) Hydrogel drug delivery system with predictable and tunable drug release and degradation rates, *Proc. Natl. Acad. Sci. USA 110*, 2318-2323.

4. Jayawickreme, C., Sauls, H., Watson, C., Moncol, D., Rimele, T., and Kenakin, T. (2005) Functional screening in the melanophore bioassay, *Curr. Protoc. Pharmacol. Chapter 12*, Unit 12.19.

5. Herring, C., Holt, L. J., Jespers, L. J., Mayer, S., and Pupecka-Swider, M. (2004) Drug fusions and conjugates, *US 8,779,103 B2*.

6. Jelsing, J., Vrang, N., Hansen, G., Raun, K., Tang-Christensen, M., and Knudsen, L. B. (2012) Liraglutide: short-lived effect on gastric emptying -- long lasting effects on body weight, *Diabetes Obes. Metab. 14*, 531-538.